Predicting PM2.5 Concentrations Across USA Using Machine Learning

P. Preetham Vignesh[1], Jonathan H Jiang[2], and Pangaluru Kishore[3]

[1]University High School
[2]Jet Propulsion Laboratory, California Institute of Technology
[3]University of California, Irvine

March 6, 2023

Abstract

Fine particulate matter with a size less than 2.5 μm (PM2.5) is increasing due to economic growth, air pollution, and forest fires in some states in the United States. Although previous studies have attempted to retrieve the spatial and temporal behavior of PM2.5 using aerosol remote sensing and geostatistical estimation methods the coarse resolution and accuracy limit these methods. In this paper the performance of machine learning models on predicting PM2.5 is assessed with Linear Regression (LR), Decision Tree (DT), Gradient Boosting Regression (GBR), AdaBoost Regression (ABR), XG Boost (XGB), k-nearest neighbors (KNN), Long Short-Term Memory (LSTM), Random Forest (RF), and support vector machine (SVM) using PM2.5 station data from 2017-2021. To compare the accuracy of all the nine machine learning models the coefficient of determination (R2), root mean square error (RMSE), Nash-Sutcliffe efficiency (NSE), root mean square error ratio (RSR), and percent bias (PBIAS) were evaluated. Among all nine models the RF and SVM models were the best for predicting PM2.5 concentrations. Comparison of the PM2.5 performance metrics displayed that the models had better predictive behavior in the western United States than that in the eastern United States.

Predicting $PM_{2.5}$ Concentrations Across USA Using Machine Learning

P. Preetham Vignesh[1], Jonathan H. Jiang[2], P. Kishore

[1.] University of California, Los Angeles, USA

[2.] Jet Propulsion Laboratory, California Institute of Technology, Pasadena, California, USA.

[3.] Retired, University of California, Irvine, USA

Correspondence: Jonathan.H.Jiang@jpl.nasa.gov

Keywords: Surface Temperature, Climate Model, Global Warming Projection

Abstract:

Fine particulate matter with a size less than 2.5 μm ($PM_{2.5}$) is increasing due to economic growth, air pollution, and forest fires in some states in the United States. Although previous studies have attempted to retrieve the spatial and temporal behavior of $PM_{2.5}$ using aerosol remote sensing and geostatistical estimation methods the coarse resolution and accuracy limit these methods. In this paper the performance of machine learning models on predicting $PM_{2.5}$ is assessed with Linear Regression (LR), Decision Tree (DT), Gradient Boosting Regression (GBR), AdaBoost Regression (ABR), XG Boost (XGB), k-nearest neighbors (KNN), Long Short-Term Memory (LSTM), Random Forest (RF), and support vector machine (SVM) using $PM_{2.5}$ station data from 2017-2021. To compare the accuracy of all the nine machine learning models the coefficient of determination (R^2), root mean square error (RMSE), Nash-Sutcliffe efficiency (NSE), root mean square error ratio (RSR), and percent bias (PBIAS) were evaluated. Among all nine models the RF and SVM models were the best for predicting $PM_{2.5}$ concentrations. Comparison of the $PM_{2.5}$ performance metrics displayed that the models had better predictive behavior in the western United States than that in the eastern United States.

1. Introduction:

Air pollution has had negative effects on human health and has interfered with social functions; particles with diameters less than 2.5 $\boldsymbol{\mu}$ m ($PM_{2.5}$) have especially been the primary pollutants in many cities in the USA. Among air pollutants, $PM_{2.5}$ is among the most harmful and can easily cross the human defense barrier, enter the lungs, and cause human disease and even death because of its small particle size and potential for long-term exposure (Wu et al., 2018; Chen et al., 2019c; Wei et al., 2019). The $PM_{2.5}$ observations were from environmental monitoring stations, however, the quantity of available $PM_{2.5}$ data presented regional differences due to the uneven station distribution.

He et al. (2016) conducted research that indicates the $PM_{2.5}$ pollution index was positively correlated with the emergency admission rate of female acute myocardial infarction and with the increased incidence of diabetes and hypertension. According to the latest urban air quality database, 98% of low and middle income countries with more than 100,000 inhabitants do not meet the World Health Organization (WHO) air quality guidelines [2].

Several researchers have used satellite remote sensing data for spatial monitoring coverage in their studies to estimate $PM_{2.5}$ concentrations (Fang et al., 2016; Hu et al., 2017; Park et al., 2019). One way of using remote sensing satellites for estimating $PM_{2.5}$ levels is through the aerosol optical depth (AOD) parameter, which refers to the solar radiation attenuation due to the scattering and absorption characteristics of aerosols within the atmosphere (Hutschison et., 2005; Van Donkelaar et al., 2010; Soni et al., 2018). Wang and Christoper (2003) was the first estimated $PM_{2.5}$ using AOD measurements from Moderate Resolution Imaging Spectrometer (MODIS). Several researchers noted that satellite AOD as well as monitoring sources and transport of aerosols are key variables in estimating $PM_{2.5}$ and air quality (Gupta and Christopher, 2009). Most have used linear regression models to correlate AOD and $PM_{2.5}$ (Gupta and Christopher, 2009). Grahremanloo et al., 2021 examined seasonal behavior of $PM_{2.5}$ over Texas using the Random Forest model. Liu et al. (2005) studied $PM_{2.5}$ levels in three different areas such as urban, suburban, and county in the Eastern United States using multiple linear regression (MLR). They concluded that the model performance may decrease since the satellite images have a relatively coarse spatial resolution since each pixel represents a large area on the ground.

The design of a model for time series prediction focuses on the application of algorithms to predict future events based on past trends. The model captures the variables with certain assumptions and represents the existing dynamic relations, summarizing them to better understand the process that produced the past data to better predict the future. Most of the above studies have used linear and

non-linear regressions to correlate various parameters with $PM_{2.5}$ concentrations over a particular region. In our study we focused on the entire United States and predicted $PM_{2.5}$ concentrations over various regions using different machine learning models.

Recently, due to an increase in the application of machine learning models to various fields in order to increase the accuracy of predictions, machine learning has also been used to predict particle concentrations (Kuremoto et al., 2014; Ong et al., 2016; Gui et al., 2020). However, the data mining does not only differ from one study to another but also in terms of classification algorithms and used features. The regression, boosting models, and deep learning-based methods display remarkable performance in time-series data processing to make predictions (Hochreiter and Schmidhuber, 1997). The estimation using traditional statistical methods requires a large amount of historical data to construct the relationship between explanatory variables and target variables (Breiman, 2001b). Since machine learning is a very promising tool to forecast pollution, we proposed applying this approach to predict $PM_{2.5}$ concentrations in the USA. The model predictions based on ML algorithms were checked by cross-validation and evaluated using appropriate metrics such as root mean square (RMSE) and mean absolute error (MAE).

Earlier studies used a limited number of statistical models, but in our study, we used nearly six machine learning models to find the best accuracy of predictions. In addition to this, our research paper took a novel approach in $PM_{2.5}$ concentration research by exploring concentrations over USA as opposed to China where many existing $PM_{2.5}$studies have already been conducted. The purpose of this paper is to present the predictions of $PM_{2.5}$ over different states over the USA. The data collection and different machine learning techniques applied in the context of time series predictions are adopted for the present study as described in Section 2. Results and discussion are given in Section 3 and finally the overall conclusions are drawn from the present study presented in Section 4.

2. Datasets:

2.1 Ground $PM_{2.5}$ Measurements:

Daily $PM_{2.5}$ observational data was collected from January 2015 to December 2021 from the openaq air quality database (https://openaq.org/). These datasets are available from nearly 1081 stations around the USA. The $PM_{2.5}$ concentrations of ground sites were taken as the dependent variable of the model. In this paper, the daily $PM_{2.5}$ concentration data of 1081 ground monitoring stations were sorted in to monthly and seasonal data from January 2015 to December 2021, and the data integrity exceeded 97%. The datasets were calibrated and quality-controlled according to national standards. Figure 1 shows the ground-level monitoring site coverage over the United States; these sites collected 7 years of daily continuous observations. From this figure, we can see that $PM_{2.5}$ monitoring sites are greater in number in the eastern part than in the western part of USA. We observed small data gaps and therefore applied linear interpolation for filling the gaps of $PM_{2.5}$ datasets. However, stations are sparsely located, therefore ground level $PM_{2.5}$ monitoring sites face difficulties in meeting the data requirements (Lin et al., 2015). As expected, the $PM_{2.5}$ concentrations were much lower at remote sites compared to urban areas, mainly due to the absence of anthropogenic sources.

This study aims to achieve the best statistical comparison of nine machine learning models: Linear Regression, K-Nearest Neighbors Regressor, Logistic Regression, Gradient Boosting Regressor, Ada Boost Regressor, Decision Tree Regressor, XG Boost, Support Vector Regressor, Random Forest, Support Vector Machine, and LSTM for estimating the $PM_{2.5}$ concentrations over the specified period. The datasets are split into 80% and 20% as training and testing datasets, respectively. The training datasets are used to build the model, and the testing dataset is used to verify the model performance of the trained model.

105 **2.2 K Nearest Neighbors (K-NN)**:

106 The K-NN model is one of the earliest ML models (reference). The K-NN model categorizes each
107 unknown instance in the training set by choosing the majority class label among its k nearest
108 neighbors. Its performance is also crucially dependent on the Euclidean distance metric used to define
109 the most immediate neighbors. After determining the Euclidean distance between the data, the
110 database samples are sorted in ascending order from the least distance (maximal similarity) to
111 maximum distance (minimal similarity) [Wu et al. 2008]. The k nearest distances are looked at, and
112 the highest occurring class label of these k nearest points to the instance is decided to be the class
113 label of the previously unknown instance in the training set. Selecting an optimal value of k becomes
114 challenging since too low of a value for k can result in overfitting while a larger value of k can cause
115 the opposite to occur.

116 **2.3 Random Forest (RF)**:

117 RF is a machine learning algorithm and was proposed by Breiman (2001); it integrates multiple
118 trees through the idea of ensemble learning, utilizes classification and regression tree (CART) as
119 learning algorithms of decision trees. The RF is a set of decision trees, where the structure of each
120 one, and the space of the variables is divided into smaller subspaces so that the data in each region is
121 as uniform as possible [Hastie et al., 2005 and Breiman, 2001]. It uses the bootstrap resampling
122 technique to randomly extract k samples (with replacement) from the original training set to generate
123 new training samples. RF uses multiple base classifiers to obtain higher accuracy classification results
124 by voting or averaging. RF excels because of its ability to leverage several different independent
125 decision trees in order to classify better, thereby reducing the error from using a single decision tree
126 because oftentimes viewing classification in independent directions can lead to lower error than a
127 single decision tree's direction.

2.4 XGBoost:

This is a highly efficient and optimized distributed gradient boosting algorithm. XGBoost supports a range of different predictive modeling problems such as classification and regression. It is trained by minimizing the loss of an objective function against a dataset, and the loss function is a critical hyperparameter which is tied directly to the type of problem being solved. Regular gradient boosting, stochastic gradient boosting, and regularized gradient boosting are the three main forms of gradient boosting. For efficiency, the system features include parallelization, distributed computing, out-of-core computing, cache optimization, and optimization of data structures to achieve the best global minimum and run time.

2.5 Long Short-Term Memory (LSTM):

LSTM is well suited for prediction based on time-series data, with better performance, to learn long-term dependency, and it deals with exploding and vanishing gradient problems [Alahi et al., 2016, Kong et al., 2017]. LSTM is superior to traditional ML methods in processing large input data and is a type of Recurrent Neural Network (RNN) [Rumelhart et al., 1986], that has been proposed to predict future outputs using past inputs. LSTM is great at processing time-series data because the $PM_{2.5}$ concentrations are time-dependent, and it can better predict future air pollution concentrations by learning features contained in past air pollution concentration time-series data.

2.6 Decision Tree (DT):

Decision Trees are one of the most commonly used machine learning models in classification and regression problems. To split a node into two or more sub-nodes DT uses mean squared error (MSE). It is a tree structure with three types of nodes. The root node is the initial node, which may get split into further nodes of the branched tree that finally leads to a terminal node (leaf node) that represents the prediction or final outcome of the model. The interior nodes and branches represent features of

151 a data set and decision rules respectively. The final prediction is the average of the value of the
152 dependent variable in that particular leaf node.

153 **2.7 Gradient Boosting Regression (GBR)**:

154 The type of boosting that combines simple models called weak learners into a single composite
155 model. Gradient boosting involves optimizing the loss function and a weak learner which makes
156 predictions. Generally, the gradient descent procedure is used to minimize a set of parameters, such
157 as coefficients in a regression equation or weights in a neural network. After estimating loss or error,
158 the weights are updated to minimize that error. Gradient Boosting algorithms minimize the bias error
159 of the model. The Gradient Boosting algorithm predicts the target variable using a regressor and Mean
160 Square Error (MSE) as the cost function (for regression problems) or predicts the target variable with
161 a classifier using a Log Loss cost function (for classification problems).

162 **2.8 Support Vector Regression (SVR)**:

163 The SVR model is widely applied to time series prediction problems. It is a novel forecasting
164 approach, which is trained independently based on the same training data with different targets. The
165 SVR can be used with functions that are linear or non-linear (called kernel functions). The linear
166 function is used for the linear regression model and evaluates results with metrics such as Root Mean
167 Square Error (RMSE) and Mean Absolute Error (MAE) to estimate the performance of the model.

168 **2.9 AdaBoost Regressor (ABR)**:

169 AdaBoost (Adaptive Boosting) is a popular technique, as it combines multiple weak classifiers to
170 build one strong classifier. The boosting approach is a class of ensembles of ML algorithms and is
171 described by Schapire (1990). Generally, the boosting approach requires a large amount of training
172 data which is not possible for many cases, and one way of mitigating this issue is by using AdaBoost
173 (Freund and Schapire, 1997). The main difference of AdaBoosting from most of the other boosting
174 approaches is in computing loss functions using relative error rather than absolute error. AdaBoost

regressor fits the data set and adjusts the weights according to the error rate of the current prediction, and reduces the bias as well as the variance for supervised learning.

2.10 Linear Regression:

Linear Regression is a great statistical tool that achieves to model and predict variables by fitting the predicted values to the observed values with a straight line or surface. This fitting process is implemented by reducing the average perpendicular distance from the straight line/surface (which are the predictions) to the observed values which oftentimes are scattered. The lower this perpendicular distance, the better the line of best fit; based on this line of best fit's equation future values can be predicted. In this case, the line of best fit's equation uses the $PM_{2.5}$ values as the dependent and output variable whereas time is the independent variable.

3.0 Results and Discussion:

Before proceeding to apply machine learning models on the $PM_{2.5}$ data we will first discuss the $PM_{2.5}$ concentrations monthly mean structures, a common method of data exploration to better understand the data and potentially adjust hyperparameters of the models. Figure 2 shows the USA monthly anomalies and quantiles for four years using daily $PM_{2.5}$ values. The monthly anomalies are in percent form, so we subtracted 100 to set the average value to zero. In addition, we estimated the anomaly to be positive or negative. Using anomalies we estimated the minimum, maximum values, the 25%, 75% quantiles, and the interquartile ranges for each month of the entire time period, and the resultant plot is shown in Figure 2. During 2018, in USA, the highest levels of $PM_{2.5}$ were observed in the inland locations and they declined nearly 20% in the year 2019. In the inland areas, $PM_{2.5}$ concentrations are primarily influenced by the secondary particles' formation resulting from the oxidation of gaseous precursors (NOx, SOx,and NH3) (South Coast Air Quality Management District, 2017). $PM_{2.5}$ concentrations show a drastic change before and during pandemic years. Before

198 pandemic years the PM2.5 concentrations are higher in the spring and summer months especially
199 towards the end of summer (August) and early fall (September) during summer years.
200 The monthly $PM_{2.5}$ concentrations are greatest in 2018 when compared to other years. The
201 positive anomalies are observed on a higher frequency in August 2018 whereas negative anomalies
202 are observed more in September 2018. This indicates that before COVID-19 the $PM_{2.5}$ concentrations
203 were a little higher than in other years throughout the USA. $PM_{2.5}$ values were also higher in the
204 Eastern USA than in Western USA (Figure not shown). The decrease was moderate (in absolute and
205 relative terms) in urban areas and progressively became lower from the urban to the rural sites. From
206 our review of recent sources, primary traffic emissions are highest at traffic sites in absolute and
207 relative terms (Masiol et al., 2015; Khan et al., 2016, Pietrogrande et al., 2016). Before proceeding
208 with applying machine learning models to the data, a preliminary statistical analysis was performed
209 for each state's $PM_{2.5}$ values and all time series values were freed of trend and outliers. This was done
210 because otherwise the time-series data values would give rise to several issues during training like
211 overfitting or significantly decreasing the performance of the model. The seasonal and annual
212 variations were removed from all states' time series data points from the entire time period. This
213 ensured stationarity in the time series data, which is a preprocessing prerequisite before applying
214 different machine learning algorithms. This is because it is better to observe statistical properties of
215 a time series which do not change over time, since statistical properties would have to be averaged
216 for the entire time period, which is not as accurate.
217 **3.1 Evaluation Parameters:**
218 For model evaluation, the errors between the estimated and true values were evaluated using
219 several evaluation indices (Chadalawada & Babovic 2017; Shahid et al., 2018; Yi et al., 2019). The
220 statistical metrics selected for comparing the performance of the models and error-values between
221 computed and observed data are evaluated by Root Mean Square Error (RMSE): square root of the

mean squared differences between observed and predicted, and suggests the dispersion of the sample. Smaller RMSE indicates better performance, and as performance decreases, the RMSE increases. The coefficient of determination (R^2) indicates the collinearity (relationship) between the observed and predicted data. The R^2 value ranges from 0 to 1 (Santhi et al., 2001 and Van Liew et al., 2003). Mean absolute error (MAE): average of the absolute differences between the observed and predicted values where a small value of MAE indicates better performance. Mean absolute percentage error (MAPE): this index indicates the ratio between errors and observations, the lower the MAPE the higher the accuracy (Chen et al., 2018). Root mean square error ratio (RSR): the ratio of the RMSE to the standard deviation of measured data (Stajkowski et al., 2020). RSR is classified into four intervals: very good ($0.0 \leq RSR \leq 0.50$), good ($0.50 < RSR \leq 0.60$), acceptable ($0.60 < RSR \leq 0.70$), and unacceptable ($RSR > 0.70$), respectively (Khosravi et al., 2018). Nash-Sutcliffe efficiency (NSE): is a normalized statistical metric to determine the relative magnitude of the residual variance relative to the variance or noise (Nash and Sutcliffe 1970). NSE performance ratings are very good ($0.75 < NSE \leq 1.0$), good ($0.65 < NSE \leq 0.75$), satisfactory ($0.50 < NSE \leq 0.65$), and unsatisfactory ($NSE \leq 0.50$). Percent bias (PBIAS): it measures the average percent of the predicted value that is smaller or larger than the observed value (Malik et al., 2018; Nury et al., 2017). The PBIAS is classified into four ranges, very good ($PBIAS < \pm 10$), good ($\pm 10 \leq PBIAS < \pm 15$), satisfactory ($\pm 15 \leq PBIAS < +25$), and unsatisfactory ($PBIAS \geq \pm 25$).

$$MSE = \frac{\sum_{i=1}^{n}\left(x_{oi} - x_{pi}\right)^2}{N}$$

$$MAE = \frac{1}{N}\sum_{i=1}^{n}\left|x_{oi} - x_{pi}\right|$$

$$R^2 = 1 - \frac{\sum_{i=1}^{n}(x_{oi} - x_{pi})^2}{\sum_{i=1}^{n}(x_{oi} - x_{mean})^2}$$

$$RSR = \frac{RMSE}{STDEV_{obj}} = \frac{\sqrt{\sum_{i=1}^{n}(x_{oi}-x_{pi})^2}}{\sqrt{\sum_{i=1}^{n}(x_{oi}-x_{mean})^2}}$$

$$PBIAS = \left|\frac{\sum_{i=1}^{n}(x_{oi}-x_{pi})}{\sum_{i=1}^{n}x_{oi}}\right| * 100$$

$$NORM = \sqrt{\sum_{i=1}^{n}(x_{oi}-x_{pi})^2}$$

$$MAPE = \frac{\sum_{i=1}^{n}\frac{|x_{oi}-x_{pi}|}{x_{oi}}}{N} * 100\%$$

$$\mathrm{NSE} = 1 - \left[\frac{\sum_{i=1}^{n}(x_{oi}-x_{pi})^2}{\sum_{i=1}^{n}(x_{oi}-x_{mean})^2}\right]$$

where N refers to the number of data points, x_{oi}, x_{pi} are the observed and predicted daily $PM_{2.5}$ concentrations, respectively.

The nine machine learning models can describe daily variations of observed and estimated values of $PM_{2.5}$ concentrations as shown in Figure 3 and Figure 4, in which the blue curve represents the observed $PM_{2.5}$ concentrations, while the red curve represents the estimated $PM_{2.5}$ concentrations. We generated time series plots for all states but we showed one state from the western side of the USA: California (Figure 3) and another state from east USA: New York (Figure 4). All nine machine learning models show that the seasonal variability of $PM_{2.5}$ concentration is lower in the spring and summer and higher in autumn and winter, maybe due to atmospheric circulation of autumn and winter. The $PM_{2.5}$ concentrations in the autumn and winter are less accurate because air pollution is more severe than that in spring and summer. The SVM and RF models give better agreement with observed $PM_{2.5}$ concentrations. However, the California $PM_{2.5}$ estimations are less accurate than those of the New York because pollution is more severe due to forest fires in the summer. Sulfate

concentrations may reflect regional influences of $PM_{2.5}$; these concentrations decreased from east to west but with higher amounts in California (Meng et al. 2018).

Figures 5 and 6 display California and New York's scatter plots of the observed vs estimated daily $PM_{2.5}$ concentrations during the period of observations using different machine learning models respectively. The scatter plot of the two variables suggests a positive linear relationship between them. All points on the scatter plot lie on a straight line; this indicates the differences are zero and suggest a strong correlation between the observed and estimated $PM_{2.5}$ concentrations. Tables 1 and 2 indicate the performance and statistical metrics as estimated for New York and California. The metrics of all models in Table 1 are for New York: Random Forest with $R^2 = 0.899$, MAE = 2.122, and RMSE = 3.121 has less error than the other models. The next model with the lowest error is Support Vector Machine with $R^2 = 0.857$, MAE = 2.145, and RMSE = 3.125.

The performance of the models at different states are good at most sites, as 73% of them show an R2 > 0.62 and 10% show an R2 less than 0.3. Moreover, an average RMSE less than 4.5 Mg/m3 in 70% of the states and more than 5 Mg/m3 in rest of the states demonstrates good performance. $PM_{2.5}$ estimations are lower and higher than observations with high and low $PM_{2.5}$ concentration scenarios respectively, indicating that estimation accuracy will decline in extreme cases in both states. Zhan et al. (2017) also found similar behavior using $PM_{2.5}$ concentration in some parts of China. This may be due to the model's lack of performanced caused by a smaller amount of training data, especially during extreme $PM_{2.5}$ concentrations. Ghahremanloo et al. 2021 observed $PM_{2.5}$ levels in Texas are maximal in the summer and are attributed to higher temperatures and humidity that accelerate the formation of nitrate and sulfate from NO2 and SO2 (Lin et al., 2019). Overall, the performance of RF is reasonable, with California's R^2, RMSE, and MAE values of 0.77, 3.051 mg/m3, and 2.233 mg/m3, respectively. New York's R^2, RMSE, and MAE values were 0.899, 3.121 mg/m3, and 2.12 mg/m3, respectively. Comparing California's to New York's results, we observe that the California $PM_{2.5}$

296 concentration values and biases were slightly higher. Overall, the average error values are slightly
297 lower in the Eastern states than in the Western states. Each state's R2, RMSE, MAE, and bias values
298 are estimated for each model and we observed RF and SVM models produce better estimates than
299 the other models. On average, the R2 of the SVM model is 5% higher than that of the RF model. The
300 biases are 15% lower in the Eastern states than in the Western states of the USA. The high sulfate
301 concentrations around Los Angeles and Long Beach may be due to the ship emissions, since these
302 two areas combined have one-fourth of all container cargo traffic in the Unites States
303 (http://www.dot.ca.gov) (Vutukuru and Dabdub, 2008). However, the $PM_{2.5}$ estimations in the
304 autumn and winter are less accurate because air pollution is more severe than that present in the spring
305 and summer. Among the nine machine learning models, only the SVM and RF models give desirable
306 results in the mildest air pollution cases. The LSTM model performs the outperformed among all
307 models, which can neither reflect the variations of $PM_{2.5}$ concentrations significantly nor estimate the
308 $PM_{2.5}$ concentrations accurately.

309 A Taylor diagram can display multiple metrics in a single plot and can be used to summarize
310 the relative skill with several states' $PM_{2.5}$ model outputs. The Taylor diagram characterizes the
311 statistical relationship between two fields (Taylor, 2001). In this paper, observed is representing the
312 values based on observations, and predicted indicates that the values were simulated by a machine
313 learning model. Figures 7 and 8 illustrate the Random Forest and Support Vector Machine of standard
314 deviation and correlation of all states of USA. Metrics of RF and SVM were computed at each state,
315 and a number was assigned to each state considered. The position of each number appearing on the
316 plot quantifies how closely model $PM_{2.5}$ values matches with different states. Consider state 50, for
317 example and its correlation is about 0.78. The centered standard deviation difference between the
318 observed and predicted patterns is proportional to the point on the x-axis identified as observed. The
319 dotted line contours indicate the normalized standard deviation values, and it can be seen that in the

case of state 50 it is centered at about 1.65. Predicted patterns that agree well with observed test data will lie nearest to the observed marked point. The state values lie near or on the observed dotted line, and it indicates a small predicted pattern difference. Some of the state values are slightly further from the observed value, it also shows that the predicted values are larger than the observed.

4. Conclusion:

In this paper, we present the prediction of $PM_{2.5}$ concentrations over USA using various machine learning algorithms with the goal of improving our understanding of the differences among them. Machine learning algorithms are new approaches for analyzing large datasets due to the computational speed and easy implementation for massive data. In this paper we studied and examined nine machine learning models (Linear Regression, Decision Tree, Gradient Boost, Ada Boost, XG Boost, K-Nearest Neighbors, LSTM, Random Forest, and SVM) and their performance in predicting $PM_{2.5}$ concentrations.

The obtained machine learning-based methods' accuracies vary in all of USA's states, but the performance of RF (California: R^2=0.77, NSE = 0.817, PBIAS=7.022, and RSR=0.355; New York: R^2=0.899, NSE=0.811, PBIAS=2.989, and RSR=0.331) and SVM (California: R^2=0.71, NSE=0.897, PBIAS=7.027, and RSR=0.424; New York: R^2= 0.857, NSE=0.280, PBIAS=3.011, and RSR=0.338) were better than the other examined methods. Moreover, it should be noted that the accuracy and performance of these machine learning methods are not constant in different climates and regions.

Both RF and SVM models' R^2 scores were between 0.71 and 0.899, RMSE scores ranged between 3.05 to 3.714, NSE values ranged between 0.811 to 0.899, PBIAS ranged between 2.989-7.027, and RSR scores ranged between 0.331-0.424 for California and New York states. These metrics revealed high model reliability and performed well for both RF and SVM and larger datasets produced better prediction results.

Our study can also contribute to limiting human health exposure risks and helping future epidemiological studies of air pollution. With the improved computational efficiency, machine learning models improved prediction performance and served as a better scientific tool for decision-makers to make sound $PM_{2.5}$ control policies. Real-time measurements of the chemical composition of $PM_{2.5}$ taken as regulatory air quality measurements are needed in the future.

Several parameters affect $PM_{2.5}$ concentrations; in the future, it is possible to improve the performance of our machine learning models with GDP per capita, urbanization data, and other atmospheric parameters which would be investigated for model development. In the United States more extensive ground monitoring is needed, as the total number of stations is 1000, suggesting the network of stations is too sparse for a large nation (See Figure 1). This becomes much more apparent in some states as also displayed in Figure 1. However, understanding the spatial and temporal distribution of each region over the United States is helpful, especially over rural areas. Considering these areas, a larger amount of data for these locations and other ground-based locations would enhance predicting $PM_{2.5}$ concentrations. Furthermore, the machine learning models can always be updated to yield better results as new data becomes available, therefore, the expansion of sources of data becomes even more important as models can be updated.

Acknowledgements: The first author (PPV) acknowledges the Jet Propulsion Laboratory (JPL) for providing him the opportunity with their summer internship program. Author JHJ conducted research at the Jet Propulsion Laboratory and California Institute of Technology under contract by NASA. We sincerely acknowledge the open air quality group for providing PM2.5 station data used in this study.

Data availability: All $PM_{2.5}$ data used for this study can be downloaded from the public website https://openaq.org. For additional questions regarding the data sharing, please contact the corresponding author at Jonathan.H.Jiang@jpl.nasa.gov.

References:

Alahi, A., K. Goel, V. Ramanathan, A. Robicquest, L. Fei-Fei, and S. Savarese, "Social LSTM: Human trajectory prediction in crowded spaces", in Proc. IEEE Conf. Comput.Vis. Pattern Recognit., Jun, 2016, pp.961-971.

Breiman, L. Random Forests, Mach. Learn. 2001, 45, 5-32. https://doi.org/1.0.1023/A: 1010933404324.

Breiman, L., 2001b, Statistical modeling: the two cultures. Stat. Sci., 16 (3), 199-215, https://doi.org/10.1214/ss/1009213726.

Chadalawada, J., and Babovic, V., 2017. Review and comparison of performance indices for automatic model induction. J. of Hydroinformatics, 21, 13-31, https://doi.org/10.2166/hydro.2017.078.

Chen, S., Li, D.C., Zhang, H.Y., Yu, D.K., Chen, R., Zhang, B., Tan, Y.F. et al., 2019c. The development of a cell-based model for the assessment of carcinogenic potential upon long-term PM2.5 exposure. Environ. Int. 131, https://doi.org/10.1016/j.envint.2019.104943.

Fang, X., Zou, B., Liu, X., Sternberg, T., Zhai, I., 2016. Satellite-based ground PM2.5 estimation using timely structure adaptive modeling. Rem. Sens. Environ, 186, 152-163.

Freund, Y., Schapire, R.E., 1997. A decision-theoritic generalization og on-line learning and an application to boosting, J. computer and Ssystem Sciences, 55 (1), 119-139.

Ghahremanloo, M., Lops, Y., Choi, Y., Mousavinezhad, S., 2021. Impact of the COVD-19 outbreak on air pollution levels in East Asia. Sci. Total Environ. 142226.

Gui, K., Che, H., Zeng, Z., Wang, Y., Zhai, S., Wang, Z., Luo, M., Zhang, L., Liao, T., Zhao, H., Li, L., Zheng, Y., Zhang, X., 2020. Construction of a virtual PM2.5 observation network in China based on high-density surface meteorological observations using the extreme gradient boosting model. Environ. Int. 141, 105801. https://doi.org/10.1016/j.envint.2020.105801.

Gupta, P., Christopher, S.A., 2009. Particulate matter air quality assessment using integrated surface, satellite, and meteorological products: 2. A neural network approach. J. Geophys. Res. Atmosphere 114 (D20).

Hastie, T,; Tibshirani, R.; Friedman, J,; Franklin, J. The elements of statistical learning: Data mining, inference and prediction. Math. Intell. 2005, 27, 83-85.

He, X. N., Chen, P., Zhang, C., Chen, J.Y. Study on the correlation between PM2.5 and onset of acute myocardial infarction among female patients. Child Care China 31, 22, 4626-4629, 2016.

Hu, X., Belle, J.H., Meng, X., Wildani, A., Waller, L.A., et al. Estimating PM2.5 concentrations in the conterminous United States using the Random Forest approach. Environ, Sci., Technol. 2017, 51, 6936-6944. https://doi.org.10.1021/acs.est.7b01210.

Hochreiter, S., and Schmidhuber, J., 1997. Long short-term memory, Neural Comput., 9, 8, 1735-1780.

Hutschison, K.D., Smith, S., Faruqui, S.J., 2005. Correlating MODIS aerosol optical thickness data with ground-based PM2.5 observations across Texas for use in a real time air-quality prediction system. Atmos. Environ. 39 (37), 7190-7203.

Lin, C., Li, Y., Yuan, Z., Lau, A.K.H., Li, C., Fung, J.C.H., 2015. Using satellite remote sensing data to estimate the high-resolution distribution of ground-level PM2.5. Remote Sens. Environ. 156, 117-128. https://doi.org/10.1016/j.rse.2014.09.015.

Khan, M.B., Masiol, M., Forementon, G., Gilio, A.D., de Gennaaro, G., Agostinelli, C., and Pavoni, B, 2016. Carboneous PM2.5 and secondary organic aerosol across the Veneto region (NE Italy). Sci. Total Environ. 542, 172-181, doi:10.1016/j.scitotenv.2015.10.103.

Khosravi, K ; Mao, L; Kisi, O; Yaseen, Z. M; Shahid, S. Quantifying hourly suspended sediment load using data mining models: case study of a glacierized Andean catchment in Chile. J. Hydrol. 2018, 567, 165-179.

414 Kong, W., Z. Y. Dong, Y. Jia, D. J. Hill, Y. Xu, and Y. Zhang. “Short-term residential load forecasting
415 based on LSTM recurrent neural network”, IEEE Trans. Smart Grid, vol. 10, no.1, pp. 841-851,
416 Jan. 2017.
417 Kuremoto, T., Kimura, S., Kobayashi, K., and Obayashi, M., 2014. Time series forecasting using a
418 deep belief networkwith restricted Boltzmann machines, Neurocomputing, 137, 47-56.
419 Liu, B,; Philip, S. Y.; Top 10 algorithms in data mining. Knowl. Inf. Syst. 2008, 14, 1-37.
420 Liu, Y., Sarnat, J.A., Kilaru, V., Jacob, D.J., Koutrakis, P., 2005. Estimating ground-level PM2.5 in
421 the eastern United States using satellite remote sensing, Environ. Sci. Technol., 39, 3269-3278.
422 Malik, A.; Kumar. A.; Kisi, O. Daily pan evaporation estimation using heuristic methods with gamma
423 test. J. Irrig. Drain. Eng. 2018, 144, 4018023.
424 Masiol, M., Benetello, F., Harrisom, R.M., Fornenton, G., Gaspari, F.D., and Pavoni, B., 2015.
425 Spatial, seasonal trends and trans-boundary transport of PM2.5 inorganic ions in the Veneto
426 region (northeastern Italy), Atmos. Environ., 117, 19-31, doi:10.1016/j.atmosenv.2015.06.044.
427 Meng, X., Garay, M.J., Diner, D.J., Kalashnikova, O.V., Xu, J., Liu, Y., 2018. Estimating PM2.5
428 speciation concentrations using prototype 4.4 km resolution misr aerosol properties over Southern
429 California, Atmos. Environ., 181, 70-81.
430 Nash J. E., Sutcliffe, J. V. River flow forecasting through conceptual models part I – A discussion of
431 principles. J. Hydrol. 1970, 10, 282-290.
432 Nury, A.H.; Hasan, K.; Alam, M. J. Bin comparative study of wavelet-ARIMA and wavelet-ANN
433 models for temperature time series data in northeastern Bangladesh. J. King. Saud. Univ. Sci.
434 2017, 29, 47-61.
435 Ong, B.T., Sugiura, K., and Zettsu, K., 2016. Dynamically pre-trained deep recurrent neural networks
436 using environmental monitoring for predicting PM2.5, Neural Comput. Appl., 27, 6, 1553-1566.

437 Park, Y., Kwon, B., Heo, J., Hu, X., Liu, Y., Moon, T. 2019. Estimating PM2.5 concentration of the
438 conterminous Unites states via interpretable convolutional neural netwoks. Environ. Pollut.
439 113395.
440 Pietrogrande, M.C., Bacco, D., Ferrari, S., Ricciardelli, I., Scotto, F., Trentini, A., and Visentin, M.:
441 2016. Characteristics and major sources of carbonaceous aerosols in PM2.5 in Emilia Romagna
442 Region (Northern Italy) from four-year observations. Sci. Total Environ., 553, 172-183,
443 doi:10.1016/j.scitotenv.2016.02.074.
444 Santhi, C; Arnold, J. G.; Williams, J. R.; Dugas, W. A; Srinivasan, R.; and Hauck, L. M. Validation
445 of the swat model on a large river basin with point and non-point sources, JAWRA. J. Am. Water
446 Resour. Assoc., 2001, 37, 1169-1188.
447 Schapire, R. (1990). The strength of weak learnability. Machine Learning, 5 (2), 197-227.
448 Freund, Y., Schpire, R (1997). A decision-theoretic generalisation of on-line learning and an
449 application of boosting. J. Computer and System Sciences, 55 (1), 119-139.
450 Soni, M., Payra, S., Verma, S., 2018. Particulate matter estimation over a semi-arid region Jaipur,
451 India using satellite AOD and meteorological parameters. Atmospheric Pollution Research 9 (5),
452 949-958.
453 Stajkowski, S; Kumar, D; Samui, P; Bonakdari, H; and Gharabaghi, B, Genetic algorithm-optimized
454 sequential model for water temperature prediction, Sustainability, 12, 13, 5374, 2020.
455 Rumelhart, D. E., G. E. Hinton, and R. J. Williams, “learning representations by back-propagating
456 errors, “Nature, Vol. 323, no.6088, pp. 533-536, 1986.
457 Taylor, K.E., Summarizing multiple aspects of model performance in a single diagram, J. Geophys.
458 Res., 106, 7183-7192, 2001.

Van Donkelaar, A., Martin, R.V., Brauer, M., Kahn, R., Levy, R., Verduzco, C., Villeneuve, P.J., 2010. Global estimates of ambient fine particulate matter concentrations from satellite-based optical depth: development and application. Environ. Health Perspect. 118 (6), 847-855.

Van Liew, M. W; Arnold, J. G.; Garbrecht, J. D. Hydrologic simulation on agricultural watersheds: Choosing between two models. Trans. ASAE 2003, 56, 1539.

Vutukuru, S., Dabdub, D., 2008. Modeling the effects of ship emissions on coastal air quality: a case study of Southern California. Atmos. Environ. 42, 3751-3764.

Wang, J., Christopher, S.A., 2003. Intercomparison between satellite-derived aerosol optical thickness and PM2.5 mass: Implications for air quality studies. Geophys. Res. Lett. 30 (21).

Wei, J., Huang, W., Li,, Z., Xue, W., Peng, Y., Sun, L., Gribb, M., 2019. Estimating 1-km resolution PM2.5 concentrations across China using space-time random forest approach. Rem. Sens. Environ. 231, 111221.

World Health Organization, media centre (2016). Air pollution levels are rising in many of the world's poorest cities: http://www.int/mediacentre/news/releases/2016/air-pollution-raising/.

Wu, X.; Kumar, V.; Quinlan, J. R.; Ghosh, J.; Yang, Q.; Motoda, H.; McLachlan, G. J.; Ng, A.;

Yi. L., Mengfan, T., Kun, Y., Yu, Z., Xiaolu, Z., Miao, Z., Yan, S., 2019. Research on PM2.5 estimation and prediction method and changing characteristics analysis under long temporal and large spatial scale – a case study in China typical regions. Sci. Total Enviro. 696, 133983, https://doi.org/10.1016/j/scitotenv.2019.133983.

Zhang, Y., Cao,F., 2015. Fine particle matter (PM2.5)in China at a city level. Sci. Rep., 5, 14884.

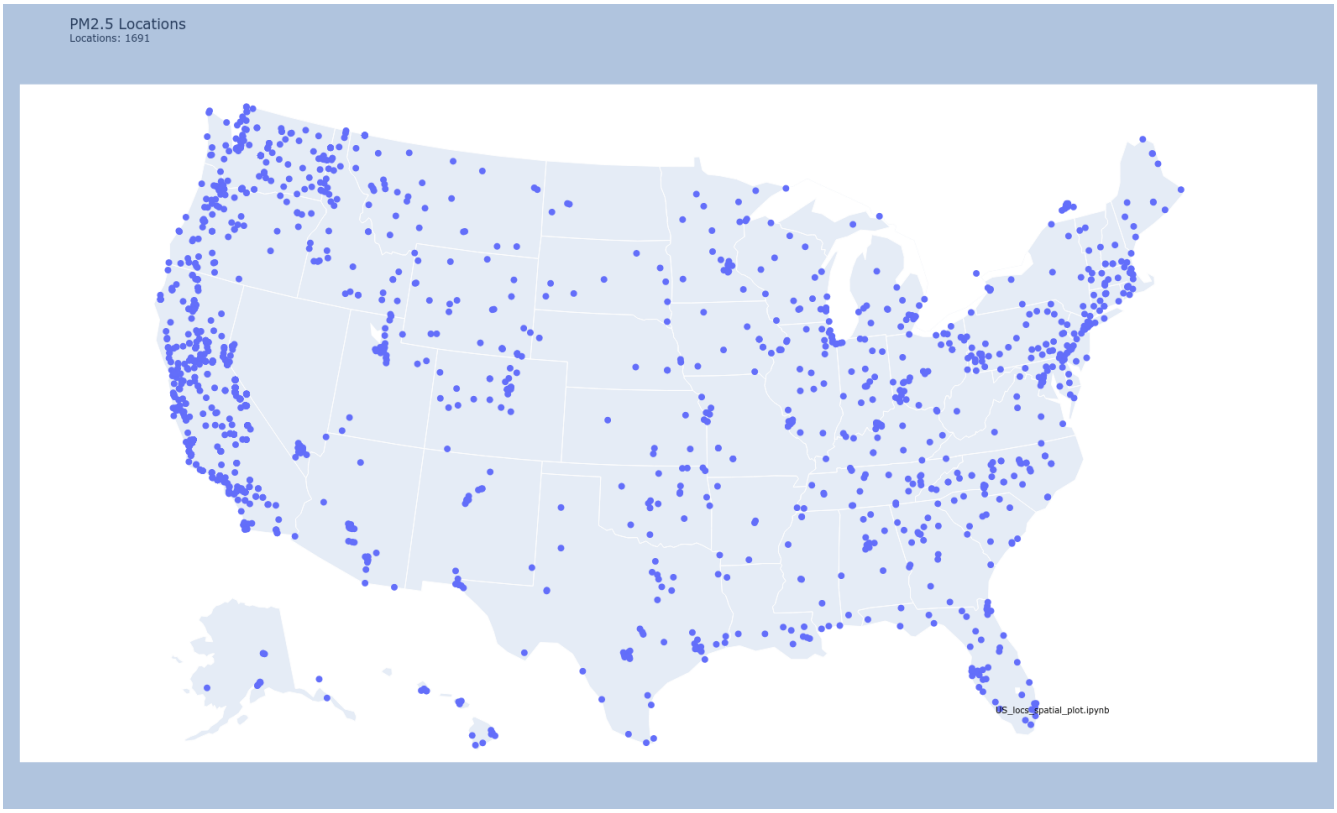

480

481 **Figure 1**. Locations of $PM_{2.5}$ monitoring sites over USA

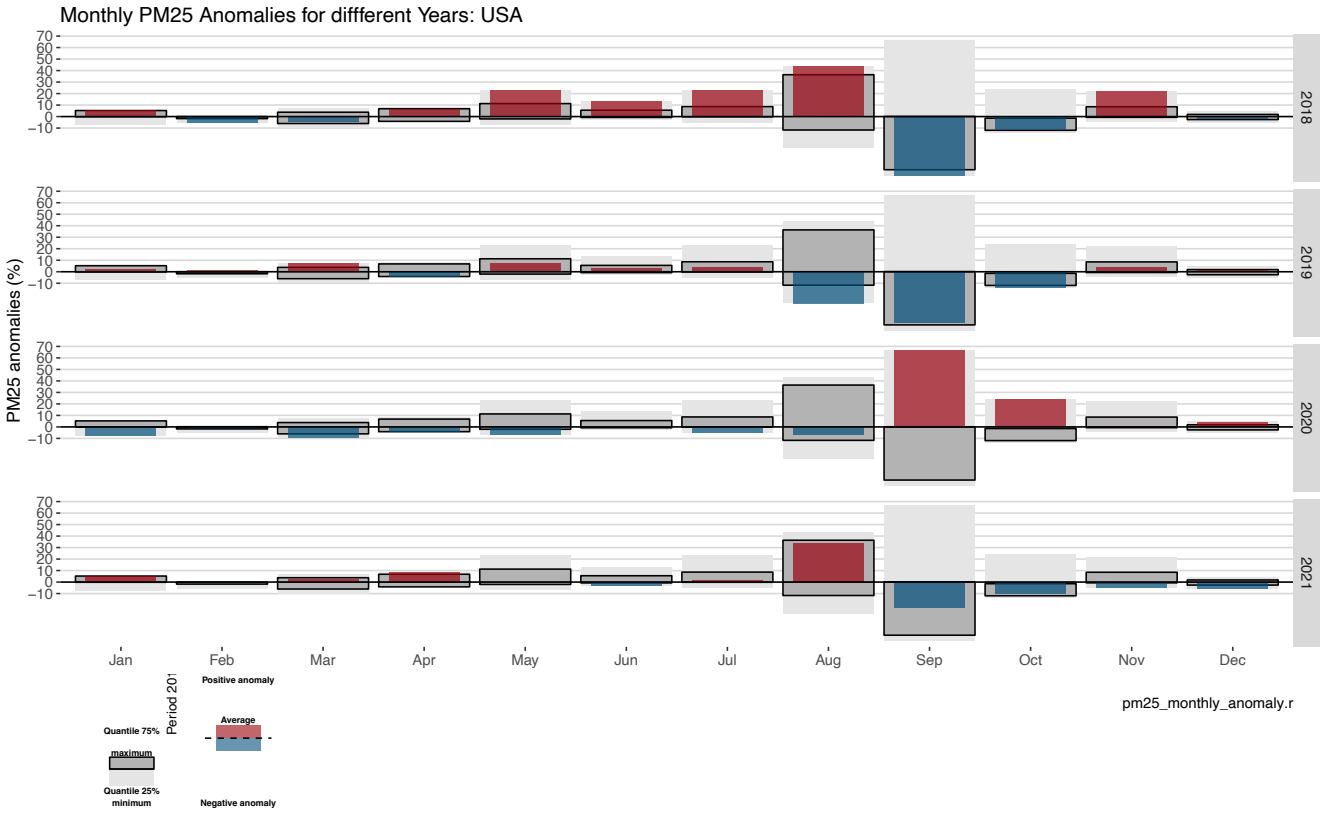

482

483 **Figure 2.** Monthly anomalies and quantiles for the observed period (2018-2021) using daily $PM_{2.5}$

484 values over United States.

485

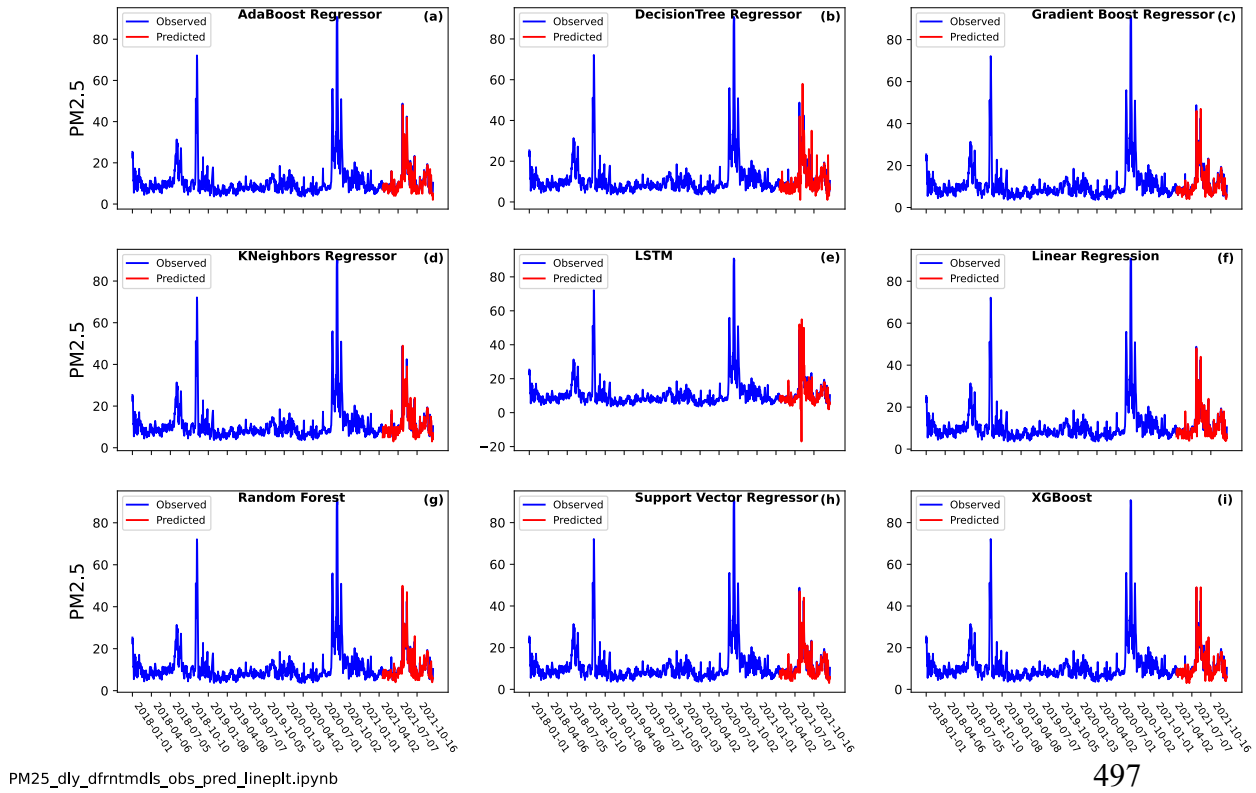

PM25_dly_dfrntmdls_obs_pred_lineplt.ipynb

Figure 3. The comparison of the time series of estimated and observed $PM_{2.5}$ concentrations over California using different machine learning models: (a) AdaBoost regressor, (b) Decision Tree regression, (c) Gradient Boost regression, (d) K-neighbors regression (e) LSTM, (f) Linear regression, (g) Random Forest, (h) Support Vector regression, and (I) XGBoost.

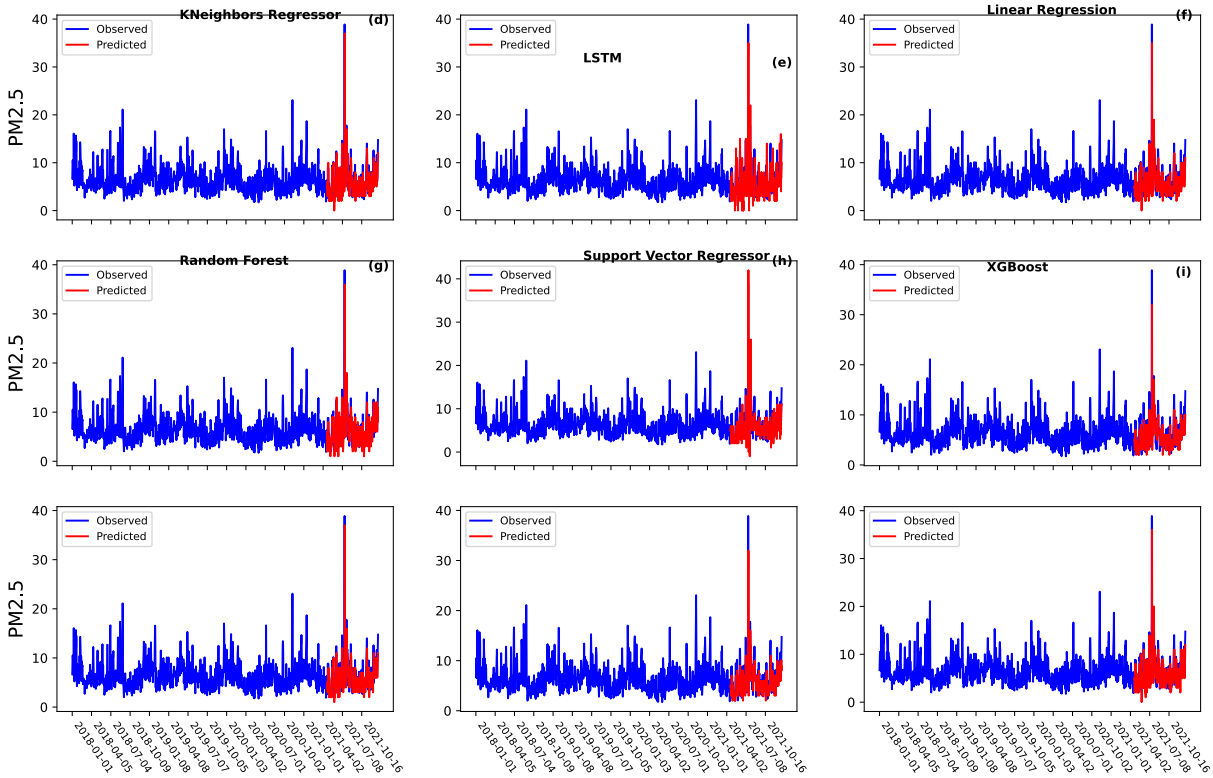

PM25_dly_dfrntmdls_obs_pred_lineplt.ipynb

503

504 **Figure 4.** The comparison of the time series of estimated and observed $PM_{2.5}$ concentrations over
505 New York using different machine learning models: (a) AdaBoost regressor, (b) DecisionTree
506 regression, (c) Gradient Boost regression, (d) Kneighbors regression (e) LSTM, (f) Linear regression,
507 (g) Random Forest, (h) Support Vector regression, and (I) XGBoost.
508

509

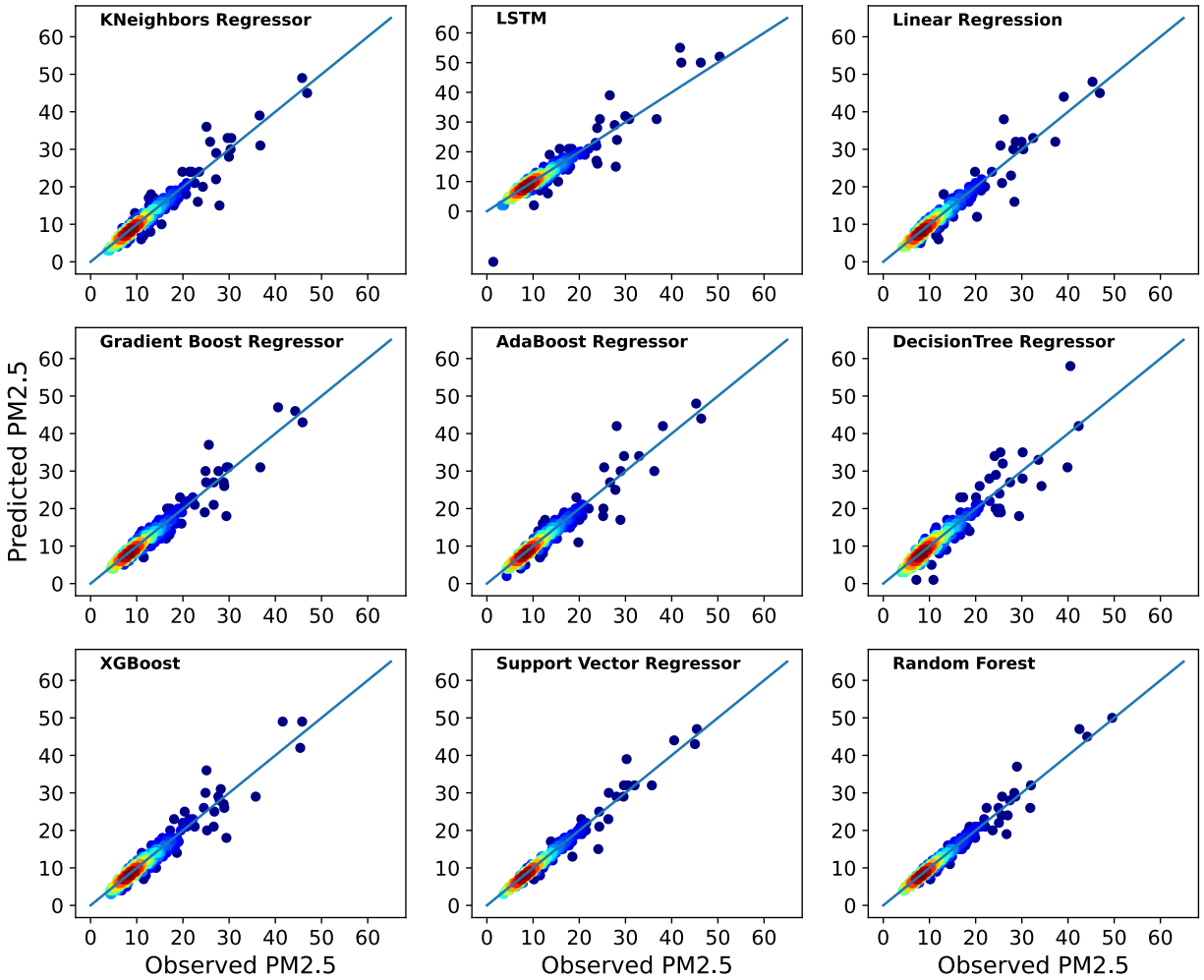

510

511 **Figure 5.** Scatter plots of observed and estimated daily $PM_{2.5}$ concentrations over California using
512 different machine learning models: (a) AdaBoost regressor, (b)DecisionTree regression, (c) Gradient
513 Boost regression, (d) Kneighbors regression (e) LSTM, (f) Linear regression, (g) Random Forest, (h)
514 Support Vector regression, and (I) XGBoost.
515

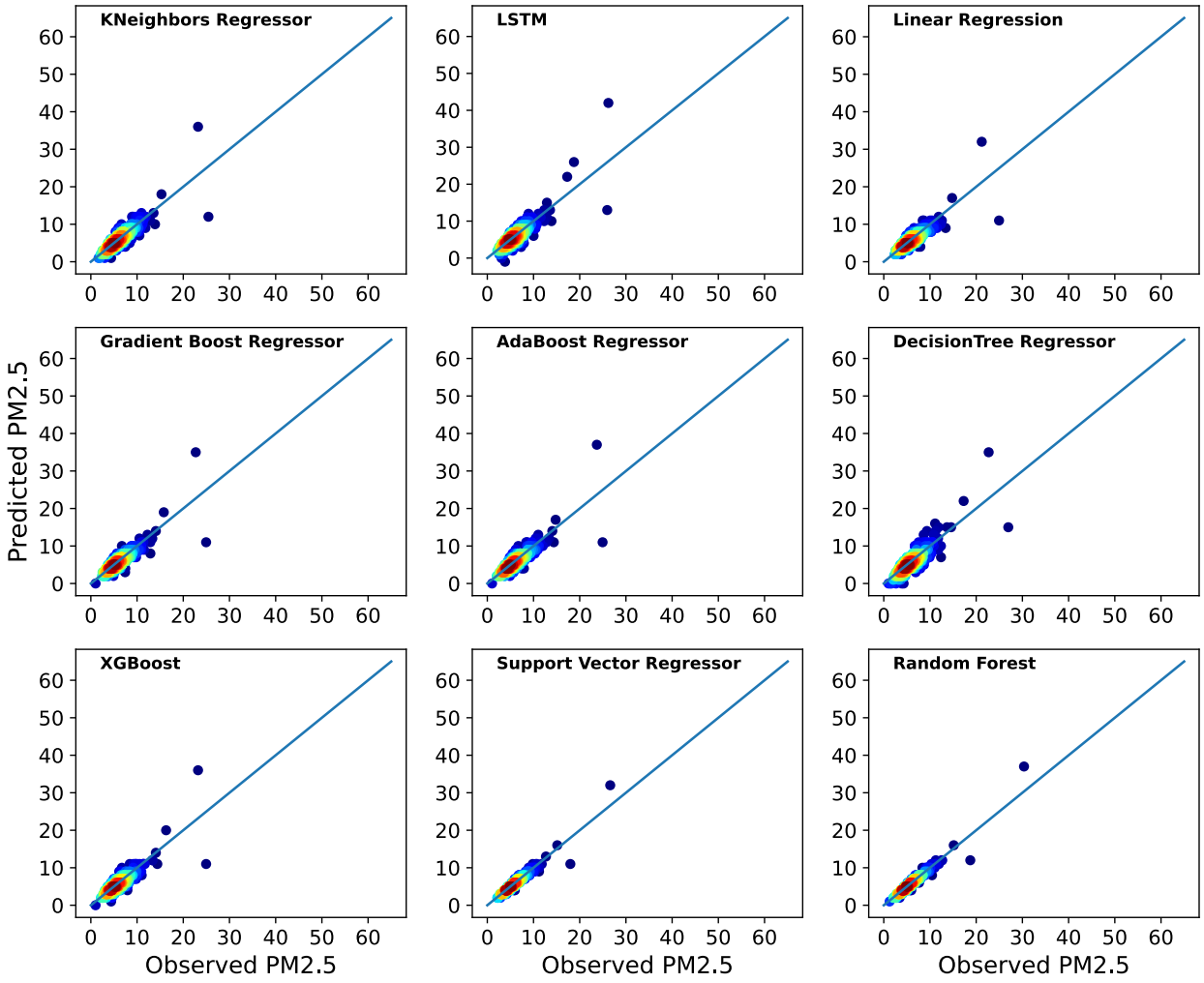

516

517 **Figure 6**. Scatter plots of observed and estimated daily $PM_{2.5}$ concentrations over New York using
518 different machine learning models: (a) AdaBoost regressor, (b)DecisionTree regression, (c) Gradient
519 Boost regression, (d) Kneighbors regression (e) LSTM, (f) Linear regression, (g) Random Forest,
520 (h) Support Vector regression, and (I) XGBoost.

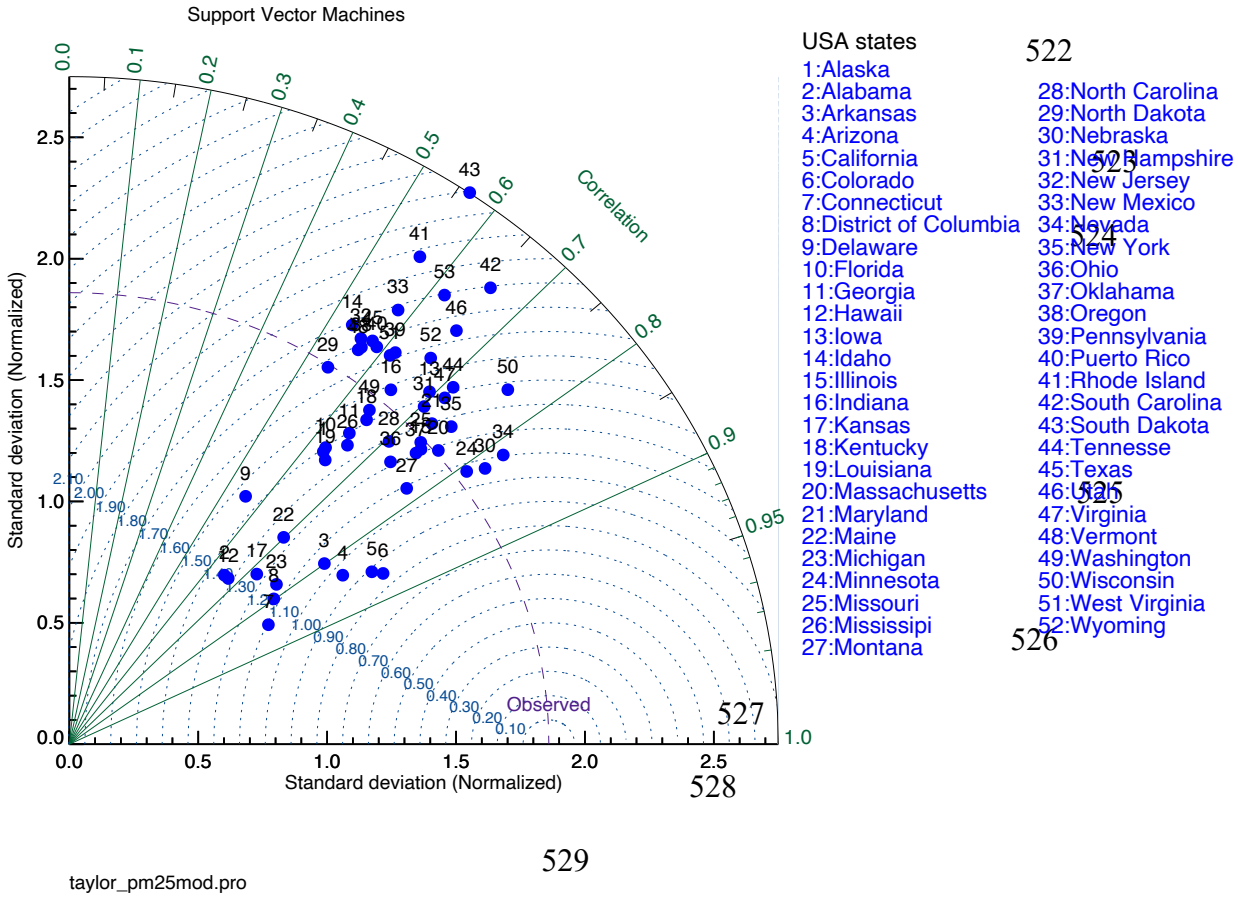

taylor_pm25mod.pro

Figure 7. Taylor diagram of the Support Vector Machines (SVM) over each state of the United States.

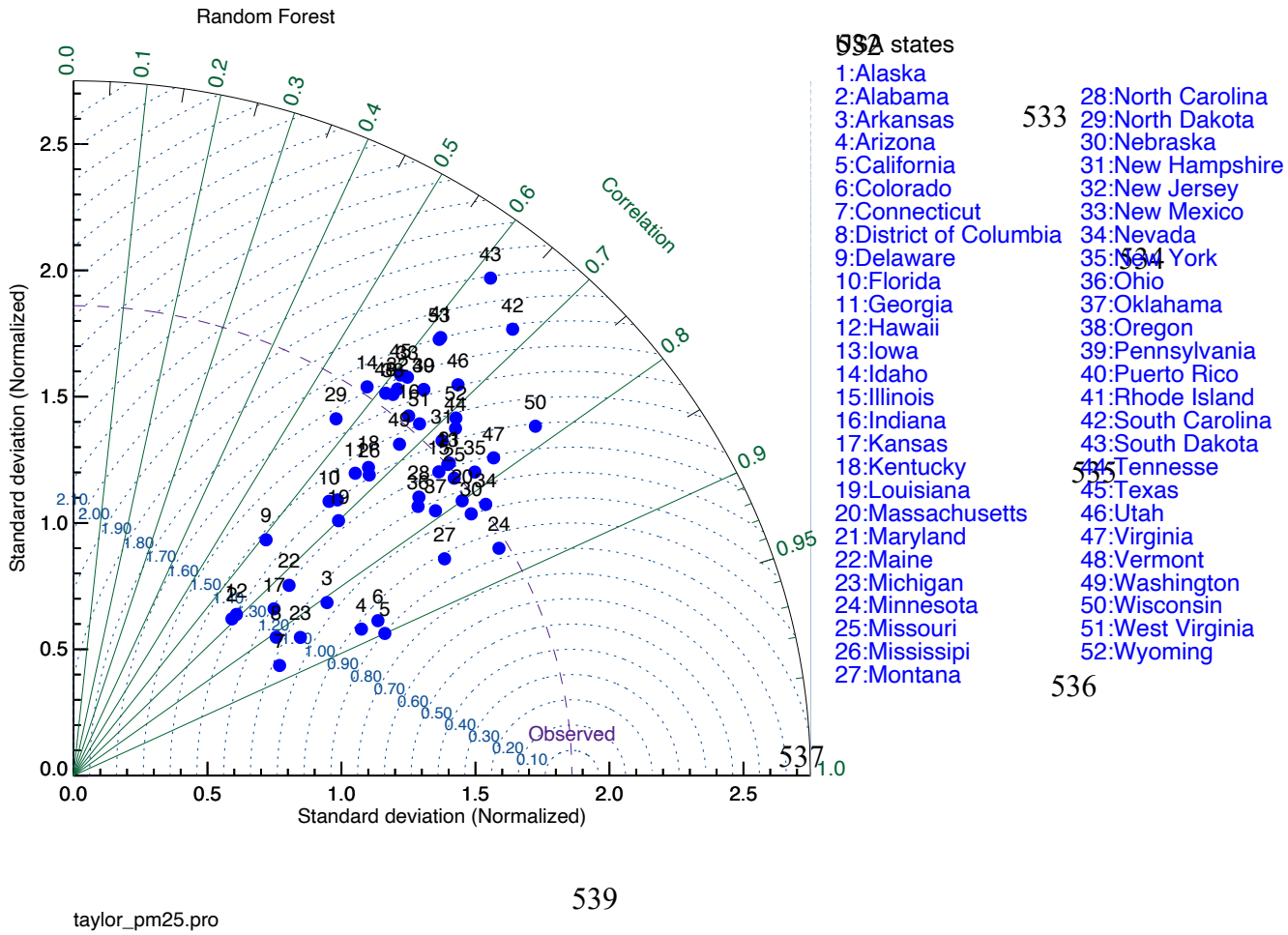

Figure 8. Taylor diagram of the Random Forest (RF) over each state of the United States.

Table 1: Different Model Metrics for New York State

New York								
Model	**RMSE**	**MAE**	**MAPE**	**R2**	**NSE**	**NORM**	**PBIAS**	**RSR**
Linear Regression	3.883	2.309	0.285	0.688	0.613	60.156	11.24	0.561
Decision Tree	5.136	3.109	0.254	0.454	0.533	79.58	13.44	0.691
Gradient Boost Regressor	3.822	2.394	0.545	0.698	0.683	59.207	8.210	0.546
AdaBoost Regressor	3.961	2.316	0.188	0.676	0.683	61.369	9.653	0.576
XG Boost	3.898	2.501	0.202	0.686	0.681	60.393	8.342	0.559
KNeighbors Regressor	3.919	2.379	0.195	0.683	0.677	60.711	7.515	0.562
LSTM	7.487	3.359	0.218	0.158	0.455	115.991	6.020	0.812
Random Forest	3.121	2.122	0.182	0.899	0.811	38.671	2.989	0.331
SVM	3.125	2.145	0.183	0.857	0.820	39.161	3.011	0.338

RMSE = Root mean squared error
MAE = Mean absolute error

MAPE = Mean absolute percentage error
R^2 = The coefficient of determination
NSE = Nash-Sutcliffe efficiency
PBIAS = Percent Bias
RSR = root mean square error ratio

Table 2: Different Model Metrics for California State

California								
Model	**RMSE**	**MAE**	**MAPE**	**R^2**	**NSE**	**NORM**	**PBIAS**	**RSR**
Linear Regression	3.695	2.599	0.326	0.43	0.694	57.243	12.086	0.932
Decision Tree	5.481	3.743	0.467	0.23	0.576	84.917	19.901	0.732
Gradient Boost Regressor	4.051	2.736	0.340	0.28	0.461	62.758	16.891	1.017
AdaBoost Regressor	3.804	2.636	0.342	0.33	0.435	58.938	17.532	0.969
XG Boost	4.271	2.972	0.372	0.17	0.438	66.178	18.726	1.075
KNeighbors Regressor	4.394	3.062	0.392	0.22	0.286	68.071	17.076	1.106
LSTM	5.025	3.252	0.339	0.46	0.309	77.853	18.027	0.618
Random Forest	3.051	2.233	0.315	0.77	0.817	46.894	7.022	0.355
SVM	3.714	2.618	0.320	0.71	0.897	47.853	7.027	0.424

RMSE = Root mean squared error
MAE = Mean absolute error
MAPE = Mean absolute percentage error
R^2 = The coefficient of determination
NSE = Nash-Sutcliffe efficiency
PBIAS = Percent Bias
RSR = root mean square error ratio

Predicting $PM_{2.5}$ Concentrations Across USA Using Machine Learning

P. Preetham Vignesh[1], Jonathan H. Jiang[2], P. Kishore

[1.] University of California, Los Angeles, USA

[2.] Jet Propulsion Laboratory, California Institute of Technology, Pasadena, California, USA.

[3.] Retired, University of California, Irvine, USA

Correspondence: Jonathan.H.Jiang@jpl.nasa.gov

Keywords: Surface Temperature, Climate Model, Global Warming Projection

Abstract:

Fine particulate matter with a size less than 2.5 μm ($PM_{2.5}$) is increasing due to economic growth, air pollution, and forest fires in some states in the United States. Although previous studies have attempted to retrieve the spatial and temporal behavior of $PM_{2.5}$ using aerosol remote sensing and geostatistical estimation methods the coarse resolution and accuracy limit these methods. In this paper the performance of machine learning models on predicting $PM_{2.5}$ is assessed with Linear Regression (LR), Decision Tree (DT), Gradient Boosting Regression (GBR), AdaBoost Regression (ABR), XG Boost (XGB), k-nearest neighbors (KNN), Long Short-Term Memory (LSTM), Random Forest (RF), and support vector machine (SVM) using $PM_{2.5}$ station data from 2017-2021. To compare the accuracy of all the nine machine learning models the coefficient of determination (R^2), root mean square error (RMSE), Nash-Sutcliffe efficiency (NSE), root mean square error ratio (RSR), and percent bias (PBIAS) were evaluated. Among all nine models the RF and SVM models were the best for predicting $PM_{2.5}$ concentrations. Comparison of the $PM_{2.5}$ performance metrics displayed that the models had better predictive behavior in the western United States than that in the eastern United States.

1. Introduction:

Air pollution has had negative effects on human health and has interfered with social functions; particles with diameters less than 2.5 $\boldsymbol{\mu}$ m ($PM_{2.5}$) have especially been the primary pollutants in many cities in the USA. Among air pollutants, $PM_{2.5}$ is among the most harmful and can easily cross the human defense barrier, enter the lungs, and cause human disease and even death because of its small particle size and potential for long-term exposure (Wu et al., 2018; Chen et al., 2019c; Wei et al., 2019). The $PM_{2.5}$ observations were from environmental monitoring stations, however, the quantity of available $PM_{2.5}$ data presented regional differences due to the uneven station distribution.

He et al. (2016) conducted research that indicates the $PM_{2.5}$ pollution index was positively correlated with the emergency admission rate of female acute myocardial infarction and with the increased incidence of diabetes and hypertension. According to the latest urban air quality database, 98% of low and middle income countries with more than 100,000 inhabitants do not meet the World Health Organization (WHO) air quality guidelines [2].

Several researchers have used satellite remote sensing data for spatial monitoring coverage in their studies to estimate $PM_{2.5}$ concentrations (Fang et al., 2016; Hu et al., 2017; Park et al., 2019). One way of using remote sensing satellites for estimating $PM_{2.5}$ levels is through the aerosol optical depth (AOD) parameter, which refers to the solar radiation attenuation due to the scattering and absorption characteristics of aerosols within the atmosphere (Hutschison et., 2005; Van Donkelaar et al., 2010; Soni et al., 2018). Wang and Christoper (2003) was the first estimated $PM_{2.5}$ using AOD measurements from Moderate Resolution Imaging Spectrometer (MODIS). Several researchers noted that satellite AOD as well as monitoring sources and transport of aerosols are key variables in estimating $PM_{2.5}$ and air quality (Gupta and Christopher, 2009). Most have used linear regression models to correlate AOD and $PM_{2.5}$ (Gupta and Christopher, 2009). Grahremanloo et al., 2021 examined seasonal behavior of $PM_{2.5}$ over Texas using the Random Forest model. Liu et al. (2005) studied $PM_{2.5}$ levels in three different areas such as urban, suburban, and county in the Eastern United States using multiple linear regression (MLR). They concluded that the model performance may decrease since the satellite images have a relatively coarse spatial resolution since each pixel represents a large area on the ground.

The design of a model for time series prediction focuses on the application of algorithms to predict future events based on past trends. The model captures the variables with certain assumptions and represents the existing dynamic relations, summarizing them to better understand the process that produced the past data to better predict the future. Most of the above studies have used linear and

non-linear regressions to correlate various parameters with $PM_{2.5}$ concentrations over a particular region. In our study we focused on the entire United States and predicted $PM_{2.5}$ concentrations over various regions using different machine learning models.

Recently, due to an increase in the application of machine learning models to various fields in order to increase the accuracy of predictions, machine learning has also been used to predict particle concentrations (Kuremoto et al., 2014; Ong et al., 2016; Gui et al., 2020). However, the data mining does not only differ from one study to another but also in terms of classification algorithms and used features. The regression, boosting models, and deep learning-based methods display remarkable performance in time-series data processing to make predictions (Hochreiter and Schmidhuber, 1997). The estimation using traditional statistical methods requires a large amount of historical data to construct the relationship between explanatory variables and target variables (Breiman, 2001b). Since machine learning is a very promising tool to forecast pollution, we proposed applying this approach to predict $PM_{2.5}$ concentrations in the USA. The model predictions based on ML algorithms were checked by cross-validation and evaluated using appropriate metrics such as root mean square (RMSE) and mean absolute error (MAE).

Earlier studies used a limited number of statistical models, but in our study, we used nearly six machine learning models to find the best accuracy of predictions. In addition to this, our research paper took a novel approach in $PM_{2.5}$ concentration research by exploring concentrations over USA as opposed to China where many existing $PM_{2.5}$studies have already been conducted. The purpose of this paper is to present the predictions of $PM_{2.5}$ over different states over the USA. The data collection and different machine learning techniques applied in the context of time series predictions are adopted for the present study as described in Section 2. Results and discussion are given in Section 3 and finally the overall conclusions are drawn from the present study presented in Section 4.

2. Datasets:

2.1 Ground $PM_{2.5}$ Measurements:

Daily $PM_{2.5}$ observational data was collected from January 2015 to December 2021 from the openaq air quality database (https://openaq.org/). These datasets are available from nearly 1081 stations around the USA. The $PM_{2.5}$ concentrations of ground sites were taken as the dependent variable of the model. In this paper, the daily $PM_{2.5}$ concentration data of 1081 ground monitoring stations were sorted in to monthly and seasonal data from January 2015 to December 2021, and the data integrity exceeded 97%. The datasets were calibrated and quality-controlled according to national standards. Figure 1 shows the ground-level monitoring site coverage over the United States; these sites collected 7 years of daily continuous observations. From this figure, we can see that $PM_{2.5}$ monitoring sites are greater in number in the eastern part than in the western part of USA. We observed small data gaps and therefore applied linear interpolation for filling the gaps of $PM_{2.5}$ datasets. However, stations are sparsely located, therefore ground level $PM_{2.5}$ monitoring sites face difficulties in meeting the data requirements (Lin et al., 2015). As expected, the $PM_{2.5}$ concentrations were much lower at remote sites compared to urban areas, mainly due to the absence of anthropogenic sources.

This study aims to achieve the best statistical comparison of nine machine learning models: Linear Regression, K-Nearest Neighbors Regressor, Logistic Regression, Gradient Boosting Regressor, Ada Boost Regressor, Decision Tree Regressor, XG Boost, Support Vector Regressor, Random Forest, Support Vector Machine, and LSTM for estimating the $PM_{2.5}$ concentrations over the specified period. The datasets are split into 80% and 20% as training and testing datasets, respectively. The training datasets are used to build the model, and the testing dataset is used to verify the model performance of the trained model.

105 **2.2 K Nearest Neighbors (K-NN)**:

106 The K-NN model is one of the earliest ML models (reference). The K-NN model categorizes each
107 unknown instance in the training set by choosing the majority class label among its k nearest
108 neighbors. Its performance is also crucially dependent on the Euclidean distance metric used to define
109 the most immediate neighbors. After determining the Euclidean distance between the data, the
110 database samples are sorted in ascending order from the least distance (maximal similarity) to
111 maximum distance (minimal similarity) [Wu et al. 2008]. The k nearest distances are looked at, and
112 the highest occurring class label of these k nearest points to the instance is decided to be the class
113 label of the previously unknown instance in the training set. Selecting an optimal value of k becomes
114 challenging since too low of a value for k can result in overfitting while a larger value of k can cause
115 the opposite to occur.

116 **2.3 Random Forest (RF)**:

117 RF is a machine learning algorithm and was proposed by Breiman (2001); it integrates multiple
118 trees through the idea of ensemble learning, utilizes classification and regression tree (CART) as
119 learning algorithms of decision trees. The RF is a set of decision trees, where the structure of each
120 one, and the space of the variables is divided into smaller subspaces so that the data in each region is
121 as uniform as possible [Hastie et al., 2005 and Breiman, 2001]. It uses the bootstrap resampling
122 technique to randomly extract k samples (with replacement) from the original training set to generate
123 new training samples. RF uses multiple base classifiers to obtain higher accuracy classification results
124 by voting or averaging. RF excels because of its ability to leverage several different independent
125 decision trees in order to classify better, thereby reducing the error from using a single decision tree
126 because oftentimes viewing classification in independent directions can lead to lower error than a
127 single decision tree's direction.

2.4 XGBoost:

This is a highly efficient and optimized distributed gradient boosting algorithm. XGBoost supports a range of different predictive modeling problems such as classification and regression. It is trained by minimizing the loss of an objective function against a dataset, and the loss function is a critical hyperparameter which is tied directly to the type of problem being solved. Regular gradient boosting, stochastic gradient boosting, and regularized gradient boosting are the three main forms of gradient boosting. For efficiency, the system features include parallelization, distributed computing, out-of-core computing, cache optimization, and optimization of data structures to achieve the best global minimum and run time.

2.5 Long Short-Term Memory (LSTM):

LSTM is well suited for prediction based on time-series data, with better performance, to learn long-term dependency, and it deals with exploding and vanishing gradient problems [Alahi et al., 2016, Kong et al., 2017]. LSTM is superior to traditional ML methods in processing large input data and is a type of Recurrent Neural Network (RNN) [Rumelhart et al., 1986], that has been proposed to predict future outputs using past inputs. LSTM is great at processing time-series data because the $PM_{2.5}$ concentrations are time-dependent, and it can better predict future air pollution concentrations by learning features contained in past air pollution concentration time-series data.

2.6 Decision Tree (DT):

Decision Trees are one of the most commonly used machine learning models in classification and regression problems. To split a node into two or more sub-nodes DT uses mean squared error (MSE). It is a tree structure with three types of nodes. The root node is the initial node, which may get split into further nodes of the branched tree that finally leads to a terminal node (leaf node) that represents the prediction or final outcome of the model. The interior nodes and branches represent features of

151 a data set and decision rules respectively. The final prediction is the average of the value of the
152 dependent variable in that particular leaf node.

153 **2.7 Gradient Boosting Regression (GBR)**:

154 The type of boosting that combines simple models called weak learners into a single composite
155 model. Gradient boosting involves optimizing the loss function and a weak learner which makes
156 predictions. Generally, the gradient descent procedure is used to minimize a set of parameters, such
157 as coefficients in a regression equation or weights in a neural network. After estimating loss or error,
158 the weights are updated to minimize that error. Gradient Boosting algorithms minimize the bias error
159 of the model. The Gradient Boosting algorithm predicts the target variable using a regressor and Mean
160 Square Error (MSE) as the cost function (for regression problems) or predicts the target variable with
161 a classifier using a Log Loss cost function (for classification problems).

162 **2.8 Support Vector Regression (SVR)**:

163 The SVR model is widely applied to time series prediction problems. It is a novel forecasting
164 approach, which is trained independently based on the same training data with different targets. The
165 SVR can be used with functions that are linear or non-linear (called kernel functions). The linear
166 function is used for the linear regression model and evaluates results with metrics such as Root Mean
167 Square Error (RMSE) and Mean Absolute Error (MAE) to estimate the performance of the model.

168 **2.9 AdaBoost Regressor (ABR)**:

169 AdaBoost (Adaptive Boosting) is a popular technique, as it combines multiple weak classifiers to
170 build one strong classifier. The boosting approach is a class of ensembles of ML algorithms and is
171 described by Schapire (1990). Generally, the boosting approach requires a large amount of training
172 data which is not possible for many cases, and one way of mitigating this issue is by using AdaBoost
173 (Freund and Schapire, 1997). The main difference of AdaBoosting from most of the other boosting
174 approaches is in computing loss functions using relative error rather than absolute error. AdaBoost

regressor fits the data set and adjusts the weights according to the error rate of the current prediction, and reduces the bias as well as the variance for supervised learning.

2.10 Linear Regression:

Linear Regression is a great statistical tool that achieves to model and predict variables by fitting the predicted values to the observed values with a straight line or surface. This fitting process is implemented by reducing the average perpendicular distance from the straight line/surface (which are the predictions) to the observed values which oftentimes are scattered. The lower this perpendicular distance, the better the line of best fit; based on this line of best fit's equation future values can be predicted. In this case, the line of best fit's equation uses the $PM_{2.5}$ values as the dependent and output variable whereas time is the independent variable.

3.0 Results and Discussion:

Before proceeding to apply machine learning models on the $PM_{2.5}$ data we will first discuss the $PM_{2.5}$ concentrations monthly mean structures, a common method of data exploration to better understand the data and potentially adjust hyperparameters of the models. Figure 2 shows the USA monthly anomalies and quantiles for four years using daily $PM_{2.5}$ values. The monthly anomalies are in percent form, so we subtracted 100 to set the average value to zero. In addition, we estimated the anomaly to be positive or negative. Using anomalies we estimated the minimum, maximum values, the 25%, 75% quantiles, and the interquartile ranges for each month of the entire time period, and the resultant plot is shown in Figure 2. During 2018, in USA, the highest levels of $PM_{2.5}$ were observed in the inland locations and they declined nearly 20% in the year 2019. In the inland areas, $PM_{2.5}$ concentrations are primarily influenced by the secondary particles' formation resulting from the oxidation of gaseous precursors (NOx, SOx,and NH3) (South Coast Air Quality Management District, 2017). $PM_{2.5}$ concentrations show a drastic change before and during pandemic years. Before

198 pandemic years the PM2.5 concentrations are higher in the spring and summer months especially
199 towards the end of summer (August) and early fall (September) during summer years.
200 The monthly $PM_{2.5}$ concentrations are greatest in 2018 when compared to other years. The
201 positive anomalies are observed on a higher frequency in August 2018 whereas negative anomalies
202 are observed more in September 2018. This indicates that before COVID-19 the $PM_{2.5}$ concentrations
203 were a little higher than in other years throughout the USA. $PM_{2.5}$ values were also higher in the
204 Eastern USA than in Western USA (Figure not shown). The decrease was moderate (in absolute and
205 relative terms) in urban areas and progressively became lower from the urban to the rural sites. From
206 our review of recent sources, primary traffic emissions are highest at traffic sites in absolute and
207 relative terms (Masiol et al., 2015; Khan et al., 2016, Pietrogrande et al., 2016). Before proceeding
208 with applying machine learning models to the data, a preliminary statistical analysis was performed
209 for each state's $PM_{2.5}$ values and all time series values were freed of trend and outliers. This was done
210 because otherwise the time-series data values would give rise to several issues during training like
211 overfitting or significantly decreasing the performance of the model. The seasonal and annual
212 variations were removed from all states' time series data points from the entire time period. This
213 ensured stationarity in the time series data, which is a preprocessing prerequisite before applying
214 different machine learning algorithms. This is because it is better to observe statistical properties of
215 a time series which do not change over time, since statistical properties would have to be averaged
216 for the entire time period, which is not as accurate.
217 **3.1 Evaluation Parameters:**
218 For model evaluation, the errors between the estimated and true values were evaluated using
219 several evaluation indices (Chadalawada & Babovic 2017; Shahid et al., 2018; Yi et al., 2019). The
220 statistical metrics selected for comparing the performance of the models and error-values between
221 computed and observed data are evaluated by Root Mean Square Error (RMSE): square root of the

mean squared differences between observed and predicted, and suggests the dispersion of the sample. Smaller RMSE indicates better performance, and as performance decreases, the RMSE increases. The coefficient of determination (R^2) indicates the collinearity (relationship) between the observed and predicted data. The R^2 value ranges from 0 to 1 (Santhi et al., 2001 and Van Liew et al., 2003). Mean absolute error (MAE): average of the absolute differences between the observed and predicted values where a small value of MAE indicates better performance. Mean absolute percentage error (MAPE): this index indicates the ratio between errors and observations, the lower the MAPE the higher the accuracy (Chen et al., 2018). Root mean square error ratio (RSR): the ratio of the RMSE to the standard deviation of measured data (Stajkowski et al., 2020). RSR is classified into four intervals: very good ($0.0 \leq RSR \leq 0.50$), good ($0.50 < RSR \leq 0.60$), acceptable ($0.60 < RSR \leq 0.70$), and unacceptable ($RSR > 0.70$), respectively (Khosravi et al., 2018). Nash-Sutcliffe efficiency (NSE): is a normalized statistical metric to determine the relative magnitude of the residual variance relative to the variance or noise (Nash and Sutcliffe 1970). NSE performance ratings are very good ($0.75 < NSE \leq 1.0$), good ($0.65 < NSE \leq 0.75$), satisfactory ($0.50 < NSE \leq 0.65$), and unsatisfactory ($NSE \leq 0.50$). Percent bias (PBIAS): it measures the average percent of the predicted value that is smaller or larger than the observed value (Malik et al., 2018; Nury et al., 2017). The PBIAS is classified into four ranges, very good ($PBIAS < \pm 10$), good ($\pm 10 \leq PBIAS < \pm 15$), satisfactory ($\pm 15 \leq PBIAS < +25$), and unsatisfactory ($PBIAS \geq \pm 25$).

$$MSE = \frac{\sum_{i=1}^{n}\left(x_{oi} - x_{pi}\right)^2}{N}$$

$$MAE = \frac{1}{N}\sum_{i=1}^{n}\left|x_{oi} - x_{pi}\right|$$

$$R^2 = 1 - \frac{\sum_{i=1}^{n}(x_{oi} - x_{pi})^2}{\sum_{i=1}^{n}(x_{oi} - x_{mean})^2}$$

$$RSR = \frac{RMSE}{STDEV_{obj}} = \frac{\sqrt{\sum_{i=1}^{n}(x_{oi}-x_{pi})^2}}{\sqrt{\sum_{i=1}^{n}(x_{oi}-x_{mean})^2}}$$

$$PBIAS = \left|\frac{\sum_{i=1}^{n}(x_{oi}-x_{pi})}{\sum_{i=1}^{n}x_{oi}}\right| * 100$$

$$NORM = \sqrt{\sum_{i=1}^{n}(x_{oi}-x_{pi})^2}$$

$$MAPE = \frac{\sum_{i=1}^{n}\frac{|x_{oi}-x_{pi}|}{x_{oi}}}{N} * 100\%$$

$$\mathrm{NSE} = 1 - \left[\frac{\sum_{i=1}^{n}(x_{oi}-x_{pi})^2}{\sum_{i=1}^{n}(x_{oi}-x_{mean})^2}\right]$$

where N refers to the number of data points, x_{oi}, x_{pi} are the observed and predicted daily $PM_{2.5}$ concentrations, respectively.

The nine machine learning models can describe daily variations of observed and estimated values of $PM_{2.5}$ concentrations as shown in Figure 3 and Figure 4, in which the blue curve represents the observed $PM_{2.5}$ concentrations, while the red curve represents the estimated $PM_{2.5}$ concentrations. We generated time series plots for all states but we showed one state from the western side of the USA: California (Figure 3) and another state from east USA: New York (Figure 4). All nine machine learning models show that the seasonal variability of $PM_{2.5}$ concentration is lower in the spring and summer and higher in autumn and winter, maybe due to atmospheric circulation of autumn and winter. The $PM_{2.5}$ concentrations in the autumn and winter are less accurate because air pollution is more severe than that in spring and summer. The SVM and RF models give better agreement with observed $PM_{2.5}$ concentrations. However, the California $PM_{2.5}$ estimations are less accurate than those of the New York because pollution is more severe due to forest fires in the summer. Sulfate

concentrations may reflect regional influences of $PM_{2.5}$; these concentrations decreased from east to west but with higher amounts in California (Meng et al. 2018).

Figures 5 and 6 display California and New York's scatter plots of the observed vs estimated daily $PM_{2.5}$ concentrations during the period of observations using different machine learning models respectively. The scatter plot of the two variables suggests a positive linear relationship between them. All points on the scatter plot lie on a straight line; this indicates the differences are zero and suggest a strong correlation between the observed and estimated $PM_{2.5}$ concentrations. Tables 1 and 2 indicate the performance and statistical metrics as estimated for New York and California. The metrics of all models in Table 1 are for New York: Random Forest with $R^2 = 0.899$, MAE = 2.122, and RMSE = 3.121 has less error than the other models. The next model with the lowest error is Support Vector Machine with $R^2 = 0.857$, MAE = 2.145, and RMSE = 3.125.

The performance of the models at different states are good at most sites, as 73% of them show an R2 > 0.62 and 10% show an R2 less than 0.3. Moreover, an average RMSE less than 4.5 Mg/m3 in 70% of the states and more than 5 Mg/m3 in rest of the states demonstrates good performance. $PM_{2.5}$ estimations are lower and higher than observations with high and low $PM_{2.5}$ concentration scenarios respectively, indicating that estimation accuracy will decline in extreme cases in both states. Zhan et al. (2017) also found similar behavior using $PM_{2.5}$ concentration in some parts of China. This may be due to the model's lack of performanced caused by a smaller amount of training data, especially during extreme $PM_{2.5}$ concentrations. Ghahremanloo et al. 2021 observed $PM_{2.5}$ levels in Texas are maximal in the summer and are attributed to higher temperatures and humidity that accelerate the formation of nitrate and sulfate from NO2 and SO2 (Lin et al., 2019). Overall, the performance of RF is reasonable, with California's R^2, RMSE, and MAE values of 0.77, 3.051 mg/m3, and 2.233 mg/m3, respectively. New York's R^2, RMSE, and MAE values were 0.899, 3.121 mg/m3, and 2.12 mg/m3, respectively. Comparing California's to New York's results, we observe that the California $PM_{2.5}$

296 concentration values and biases were slightly higher. Overall, the average error values are slightly
297 lower in the Eastern states than in the Western states. Each state's R2, RMSE, MAE, and bias values
298 are estimated for each model and we observed RF and SVM models produce better estimates than
299 the other models. On average, the R2 of the SVM model is 5% higher than that of the RF model. The
300 biases are 15% lower in the Eastern states than in the Western states of the USA. The high sulfate
301 concentrations around Los Angeles and Long Beach may be due to the ship emissions, since these
302 two areas combined have one-fourth of all container cargo traffic in the Unites States
303 (http://www.dot.ca.gov) (Vutukuru and Dabdub, 2008). However, the $PM_{2.5}$ estimations in the
304 autumn and winter are less accurate because air pollution is more severe than that present in the spring
305 and summer. Among the nine machine learning models, only the SVM and RF models give desirable
306 results in the mildest air pollution cases. The LSTM model performs the outperformed among all
307 models, which can neither reflect the variations of $PM_{2.5}$ concentrations significantly nor estimate the
308 $PM_{2.5}$ concentrations accurately.

309 A Taylor diagram can display multiple metrics in a single plot and can be used to summarize
310 the relative skill with several states' $PM_{2.5}$ model outputs. The Taylor diagram characterizes the
311 statistical relationship between two fields (Taylor, 2001). In this paper, observed is representing the
312 values based on observations, and predicted indicates that the values were simulated by a machine
313 learning model. Figures 7 and 8 illustrate the Random Forest and Support Vector Machine of standard
314 deviation and correlation of all states of USA. Metrics of RF and SVM were computed at each state,
315 and a number was assigned to each state considered. The position of each number appearing on the
316 plot quantifies how closely model $PM_{2.5}$ values matches with different states. Consider state 50, for
317 example and its correlation is about 0.78. The centered standard deviation difference between the
318 observed and predicted patterns is proportional to the point on the x-axis identified as observed. The
319 dotted line contours indicate the normalized standard deviation values, and it can be seen that in the

case of state 50 it is centered at about 1.65. Predicted patterns that agree well with observed test data will lie nearest to the observed marked point. The state values lie near or on the observed dotted line, and it indicates a small predicted pattern difference. Some of the state values are slightly further from the observed value, it also shows that the predicted values are larger than the observed.

4. Conclusion:

In this paper, we present the prediction of $PM_{2.5}$ concentrations over USA using various machine learning algorithms with the goal of improving our understanding of the differences among them. Machine learning algorithms are new approaches for analyzing large datasets due to the computational speed and easy implementation for massive data. In this paper we studied and examined nine machine learning models (Linear Regression, Decision Tree, Gradient Boost, Ada Boost, XG Boost, K-Nearest Neighbors, LSTM, Random Forest, and SVM) and their performance in predicting $PM_{2.5}$ concentrations.

The obtained machine learning-based methods' accuracies vary in all of USA's states, but the performance of RF (California: R^2=0.77, NSE = 0.817, PBIAS=7.022, and RSR=0.355; New York: R^2=0.899, NSE=0.811, PBIAS=2.989, and RSR=0.331) and SVM (California: R^2=0.71, NSE=0.897, PBIAS=7.027, and RSR=0.424; New York: R^2= 0.857, NSE=0.280, PBIAS=3.011, and RSR=0.338) were better than the other examined methods. Moreover, it should be noted that the accuracy and performance of these machine learning methods are not constant in different climates and regions.

Both RF and SVM models' R^2 scores were between 0.71 and 0.899, RMSE scores ranged between 3.05 to 3.714, NSE values ranged between 0.811 to 0.899, PBIAS ranged between 2.989-7.027, and RSR scores ranged between 0.331-0.424 for California and New York states. These metrics revealed high model reliability and performed well for both RF and SVM and larger datasets produced better prediction results.

Our study can also contribute to limiting human health exposure risks and helping future epidemiological studies of air pollution. With the improved computational efficiency, machine learning models improved prediction performance and served as a better scientific tool for decision-makers to make sound $PM_{2.5}$ control policies. Real-time measurements of the chemical composition of $PM_{2.5}$ taken as regulatory air quality measurements are needed in the future.

Several parameters affect $PM_{2.5}$ concentrations; in the future, it is possible to improve the performance of our machine learning models with GDP per capita, urbanization data, and other atmospheric parameters which would be investigated for model development. In the United States more extensive ground monitoring is needed, as the total number of stations is 1000, suggesting the network of stations is too sparse for a large nation (See Figure 1). This becomes much more apparent in some states as also displayed in Figure 1. However, understanding the spatial and temporal distribution of each region over the United States is helpful, especially over rural areas. Considering these areas, a larger amount of data for these locations and other ground-based locations would enhance predicting $PM_{2.5}$ concentrations. Furthermore, the machine learning models can always be updated to yield better results as new data becomes available, therefore, the expansion of sources of data becomes even more important as models can be updated.

Acknowledgements: The first author (PPV) acknowledges the Jet Propulsion Laboratory (JPL) for providing him the opportunity with their summer internship program. Author JHJ conducted research at the Jet Propulsion Laboratory and California Institute of Technology under contract by NASA. We sincerely acknowledge the open air quality group for providing PM2.5 station data used in this study.

Data availability: All $PM_{2.5}$ data used for this study can be downloaded from the public website https://openaq.org. For additional questions regarding the data sharing, please contact the corresponding author at Jonathan.H.Jiang@jpl.nasa.gov.

References:

Alahi, A., K. Goel, V. Ramanathan, A. Robicquest, L. Fei-Fei, and S. Savarese, "Social LSTM: Human trajectory prediction in crowded spaces", in Proc. IEEE Conf. Comput.Vis. Pattern Recognit., Jun, 2016, pp.961-971.

Breiman, L. Random Forests, Mach. Learn. 2001, 45, 5-32. https://doi.org/1.0.1023/A: 1010933404324.

Breiman, L., 2001b, Statistical modeling: the two cultures. Stat. Sci., 16 (3), 199-215, https://doi.org/10.1214/ss/1009213726.

Chadalawada, J., and Babovic, V., 2017. Review and comparison of performance indices for automatic model induction. J. of Hydroinformatics, 21, 13-31, https://doi.org/10.2166/hydro.2017.078.

Chen, S., Li, D.C., Zhang, H.Y., Yu, D.K., Chen, R., Zhang, B., Tan, Y.F. et al., 2019c. The development of a cell-based model for the assessment of carcinogenic potential upon long-term PM2.5 exposure. Environ. Int. 131, https://doi.org/10.1016/j.envint.2019.104943.

Fang, X., Zou, B., Liu, X., Sternberg, T., Zhai, I., 2016. Satellite-based ground PM2.5 estimation using timely structure adaptive modeling. Rem. Sens. Environ, 186, 152-163.

Freund, Y., Schapire, R.E., 1997. A decision-theoritic generalization og on-line learning and an application to boosting, J. computer and Ssystem Sciences, 55 (1), 119-139.

Ghahremanloo, M., Lops, Y., Choi, Y., Mousavinezhad, S., 2021. Impact of the COVD-19 outbreak on air pollution levels in East Asia. Sci. Total Environ. 142226.

Gui, K., Che, H., Zeng, Z., Wang, Y., Zhai, S., Wang, Z., Luo, M., Zhang, L., Liao, T., Zhao, H., Li, L., Zheng, Y., Zhang, X., 2020. Construction of a virtual PM2.5 observation network in China based on high-density surface meteorological observations using the extreme gradient boosting model. Environ. Int. 141, 105801. https://doi.org/10.1016/j.envint.2020.105801.

Gupta, P., Christopher, S.A., 2009. Particulate matter air quality assessment using integrated surface, satellite, and meteorological products: 2. A neural network approach. J. Geophys. Res. Atmosphere 114 (D20).

Hastie, T,; Tibshirani, R.; Friedman, J,; Franklin, J. The elements of statistical learning: Data mining, inference and prediction. Math. Intell. 2005, 27, 83-85.

He, X. N., Chen, P., Zhang, C., Chen, J.Y. Study on the correlation between PM2.5 and onset of acute myocardial infarction among female patients. Child Care China 31, 22, 4626-4629, 2016.

Hu, X., Belle, J.H., Meng, X., Wildani, A., Waller, L.A., et al. Estimating PM2.5 concentrations in the conterminous United States using the Random Forest approach. Environ, Sci., Technol. 2017, 51, 6936-6944. https://doi.org.10.1021/acs.est.7b01210.

Hochreiter, S., and Schmidhuber, J., 1997. Long short-term memory, Neural Comput., 9, 8, 1735-1780.

Hutschison, K.D., Smith, S., Faruqui, S.J., 2005. Correlating MODIS aerosol optical thickness data with ground-based PM2.5 observations across Texas for use in a real time air-quality prediction system. Atmos. Environ. 39 (37), 7190-7203.

Lin, C., Li, Y., Yuan, Z., Lau, A.K.H., Li, C., Fung, J.C.H., 2015. Using satellite remote sensing data to estimate the high-resolution distribution of ground-level PM2.5. Remote Sens. Environ. 156, 117-128. https://doi.org/10.1016/j.rse.2014.09.015.

Khan, M.B., Masiol, M., Forementon, G., Gilio, A.D., de Gennaaro, G., Agostinelli, C., and Pavoni, B, 2016. Carboneous PM2.5 and secondary organic aerosol across the Veneto region (NE Italy). Sci. Total Environ. 542, 172-181, doi:10.1016/j.scitotenv.2015.10.103.

Khosravi, K ; Mao, L; Kisi, O; Yaseen, Z. M; Shahid, S. Quantifying hourly suspended sediment load using data mining models: case study of a glacierized Andean catchment in Chile. J. Hydrol. 2018, 567, 165-179.

414 Kong, W., Z. Y. Dong, Y. Jia, D. J. Hill, Y. Xu, and Y. Zhang. “Short-term residential load forecasting
415 based on LSTM recurrent neural network”, IEEE Trans. Smart Grid, vol. 10, no.1, pp. 841-851,
416 Jan. 2017.
417 Kuremoto, T., Kimura, S., Kobayashi, K., and Obayashi, M., 2014. Time series forecasting using a
418 deep belief networkwith restricted Boltzmann machines, Neurocomputing, 137, 47-56.
419 Liu, B,; Philip, S. Y.; Top 10 algorithms in data mining. Knowl. Inf. Syst. 2008, 14, 1-37.
420 Liu, Y., Sarnat, J.A., Kilaru, V., Jacob, D.J., Koutrakis, P., 2005. Estimating ground-level PM2.5 in
421 the eastern United States using satellite remote sensing, Environ. Sci. Technol., 39, 3269-3278.
422 Malik, A.; Kumar. A.; Kisi, O. Daily pan evaporation estimation using heuristic methods with gamma
423 test. J. Irrig. Drain. Eng. 2018, 144, 4018023.
424 Masiol, M., Benetello, F., Harrisom, R.M., Fornenton, G., Gaspari, F.D., and Pavoni, B., 2015.
425 Spatial, seasonal trends and trans-boundary transport of PM2.5 inorganic ions in the Veneto
426 region (northeastern Italy), Atmos. Environ., 117, 19-31, doi:10.1016/j.atmosenv.2015.06.044.
427 Meng, X., Garay, M.J., Diner, D.J., Kalashnikova, O.V., Xu, J., Liu, Y., 2018. Estimating PM2.5
428 speciation concentrations using prototype 4.4 km resolution misr aerosol properties over Southern
429 California, Atmos. Environ., 181, 70-81.
430 Nash J. E., Sutcliffe, J. V. River flow forecasting through conceptual models part I – A discussion of
431 principles. J. Hydrol. 1970, 10, 282-290.
432 Nury, A.H.; Hasan, K.; Alam, M. J. Bin comparative study of wavelet-ARIMA and wavelet-ANN
433 models for temperature time series data in northeastern Bangladesh. J. King. Saud. Univ. Sci.
434 2017, 29, 47-61.
435 Ong, B.T., Sugiura, K., and Zettsu, K., 2016. Dynamically pre-trained deep recurrent neural networks
436 using environmental monitoring for predicting PM2.5, Neural Comput. Appl., 27, 6, 1553-1566.

437 Park, Y., Kwon, B., Heo, J., Hu, X., Liu, Y., Moon, T. 2019. Estimating PM2.5 concentration of the
438 conterminous Unites states via interpretable convolutional neural netwoks. Environ. Pollut.
439 113395.
440 Pietrogrande, M.C., Bacco, D., Ferrari, S., Ricciardelli, I., Scotto, F., Trentini, A., and Visentin, M.:
441 2016. Characteristics and major sources of carbonaceous aerosols in PM2.5 in Emilia Romagna
442 Region (Northern Italy) from four-year observations. Sci. Total Environ., 553, 172-183,
443 doi:10.1016/j.scitotenv.2016.02.074.
444 Santhi, C; Arnold, J. G.; Williams, J. R.; Dugas, W. A; Srinivasan, R.; and Hauck, L. M. Validation
445 of the swat model on a large river basin with point and non-point sources, JAWRA. J. Am. Water
446 Resour. Assoc., 2001, 37, 1169-1188.
447 Schapire, R. (1990). The strength of weak learnability. Machine Learning, 5 (2), 197-227.
448 Freund, Y., Schpire, R (1997). A decision-theoretic generalisation of on-line learning and an
449 application of boosting. J. Computer and System Sciences, 55 (1), 119-139.
450 Soni, M., Payra, S., Verma, S., 2018. Particulate matter estimation over a semi-arid region Jaipur,
451 India using satellite AOD and meteorological parameters. Atmospheric Pollution Research 9 (5),
452 949-958.
453 Stajkowski, S; Kumar, D; Samui, P; Bonakdari, H; and Gharabaghi, B, Genetic algorithm-optimized
454 sequential model for water temperature prediction, Sustainability, 12, 13, 5374, 2020.
455 Rumelhart, D. E., G. E. Hinton, and R. J. Williams, “learning representations by back-propagating
456 errors, “Nature, Vol. 323, no.6088, pp. 533-536, 1986.
457 Taylor, K.E., Summarizing multiple aspects of model performance in a single diagram, J. Geophys.
458 Res., 106, 7183-7192, 2001.

Van Donkelaar, A., Martin, R.V., Brauer, M., Kahn, R., Levy, R., Verduzco, C., Villeneuve, P.J., 2010. Global estimates of ambient fine particulate matter concentrations from satellite-based optical depth: development and application. Environ. Health Perspect. 118 (6), 847-855.

Van Liew, M. W; Arnold, J. G.; Garbrecht, J. D. Hydrologic simulation on agricultural watersheds: Choosing between two models. Trans. ASAE 2003, 56, 1539.

Vutukuru, S., Dabdub, D., 2008. Modeling the effects of ship emissions on coastal air quality: a case study of Southern California. Atmos. Environ. 42, 3751-3764.

Wang, J., Christopher, S.A., 2003. Intercomparison between satellite-derived aerosol optical thickness and PM2.5 mass: Implications for air quality studies. Geophys. Res. Lett. 30 (21).

Wei, J., Huang, W., Li,, Z., Xue, W., Peng, Y., Sun, L., Gribb, M., 2019. Estimating 1-km resolution PM2.5 concentrations across China using space-time random forest approach. Rem. Sens. Environ. 231, 111221.

World Health Organization, media centre (2016). Air pollution levels are rising in many of the world's poorest cities: http://www.int/mediacentre/news/releases/2016/air-pollution-raising/.

Wu, X.; Kumar, V.; Quinlan, J. R.; Ghosh, J.; Yang, Q.; Motoda, H.; McLachlan, G. J.; Ng, A.;

Yi. L., Mengfan, T., Kun, Y., Yu, Z., Xiaolu, Z., Miao, Z., Yan, S., 2019. Research on PM2.5 estimation and prediction method and changing characteristics analysis under long temporal and large spatial scale – a case study in China typical regions. Sci. Total Enviro. 696, 133983, https://doi.org/10.1016/j/scitotenv.2019.133983.

Zhang, Y., Cao,F., 2015. Fine particle matter (PM2.5)in China at a city level. Sci. Rep., 5, 14884.

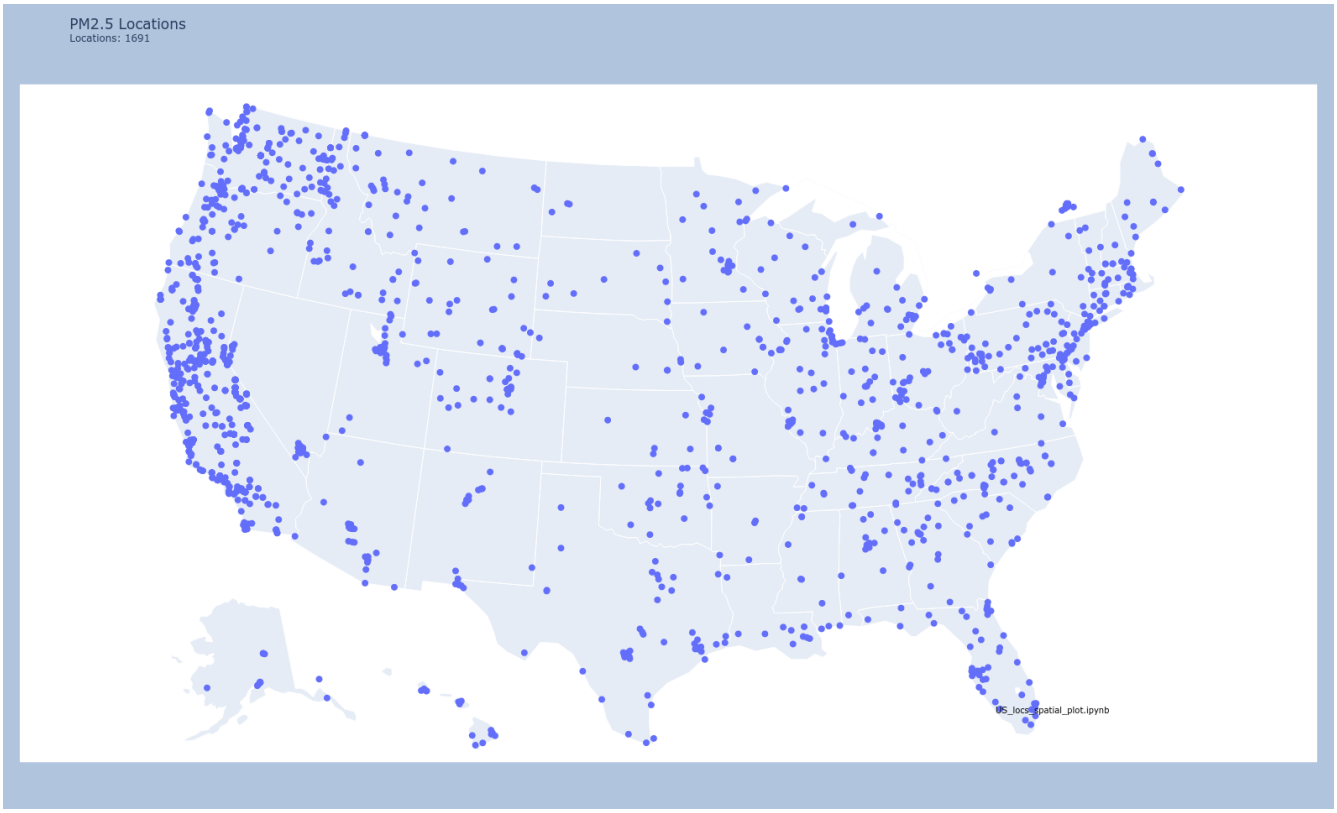

480

481 **Figure 1**. Locations of $PM_{2.5}$ monitoring sites over USA

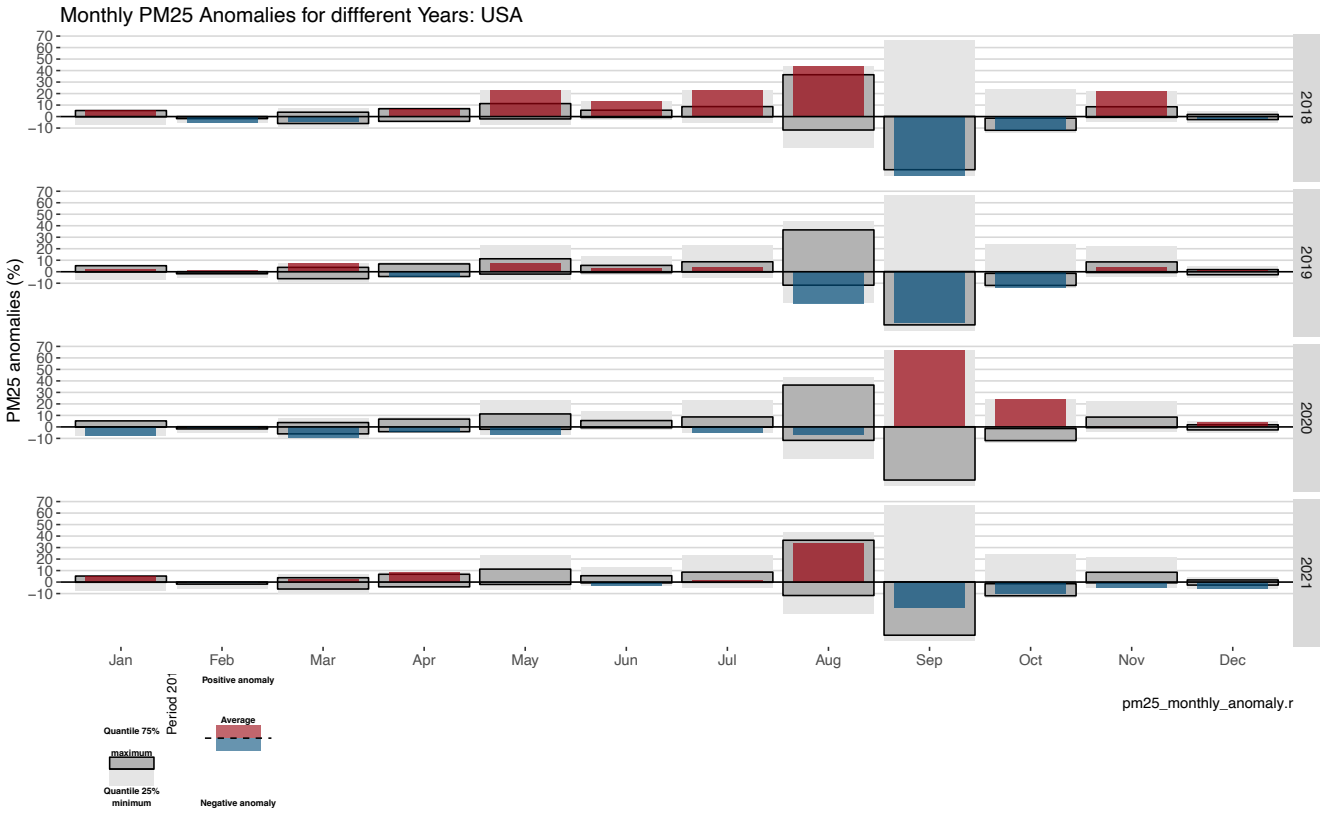

482

483 **Figure 2.** Monthly anomalies and quantiles for the observed period (2018-2021) using daily $PM_{2.5}$

484 values over United States.

485

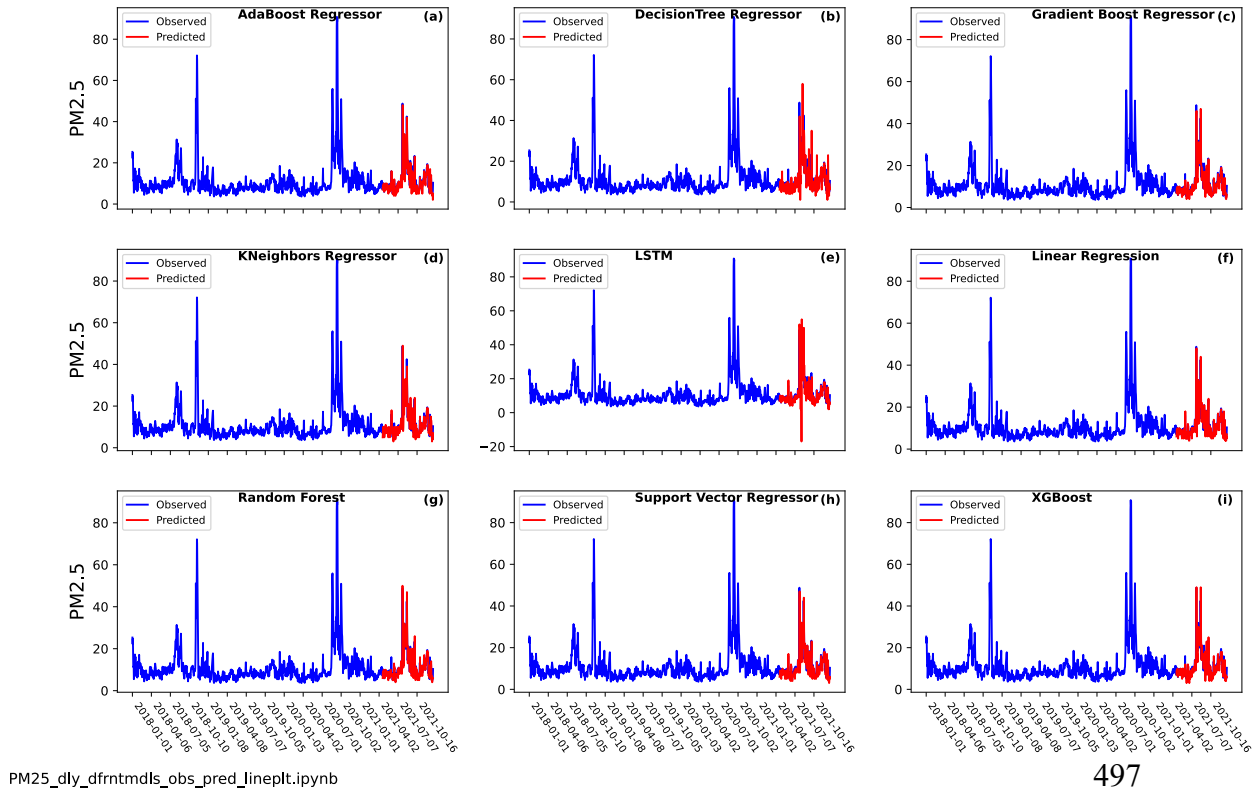

PM25_dly_dfrntmdls_obs_pred_lineplt.ipynb

Figure 3. The comparison of the time series of estimated and observed $PM_{2.5}$ concentrations over California using different machine learning models: (a) AdaBoost regressor, (b) Decision Tree regression, (c) Gradient Boost regression, (d) K-neighbors regression (e) LSTM, (f) Linear regression, (g) Random Forest, (h) Support Vector regression, and (I) XGBoost.

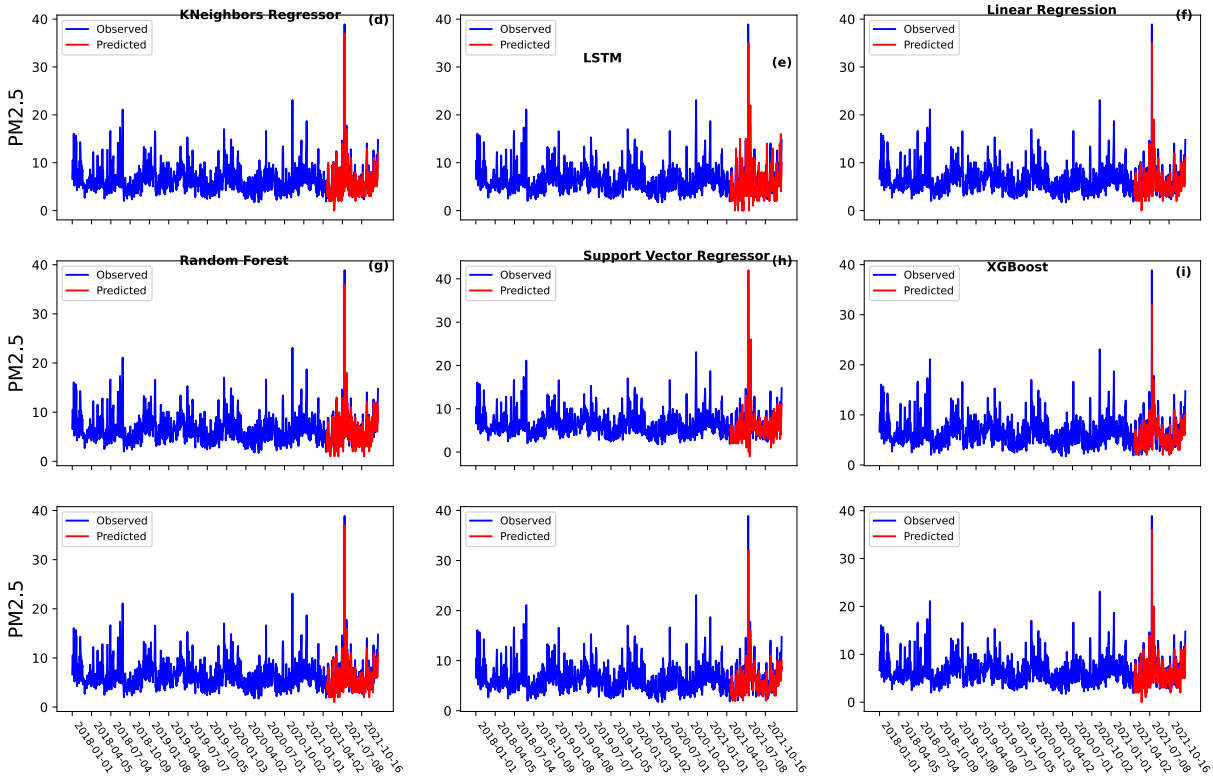

PM25_dly_dfrntmdls_obs_pred_lineplt.ipynb

503

504 **Figure 4.** The comparison of the time series of estimated and observed $PM_{2.5}$ concentrations over
505 New York using different machine learning models: (a) AdaBoost regressor, (b) DecisionTree
506 regression, (c) Gradient Boost regression, (d) Kneighbors regression (e) LSTM, (f) Linear regression,
507 (g) Random Forest, (h) Support Vector regression, and (I) XGBoost.
508

509

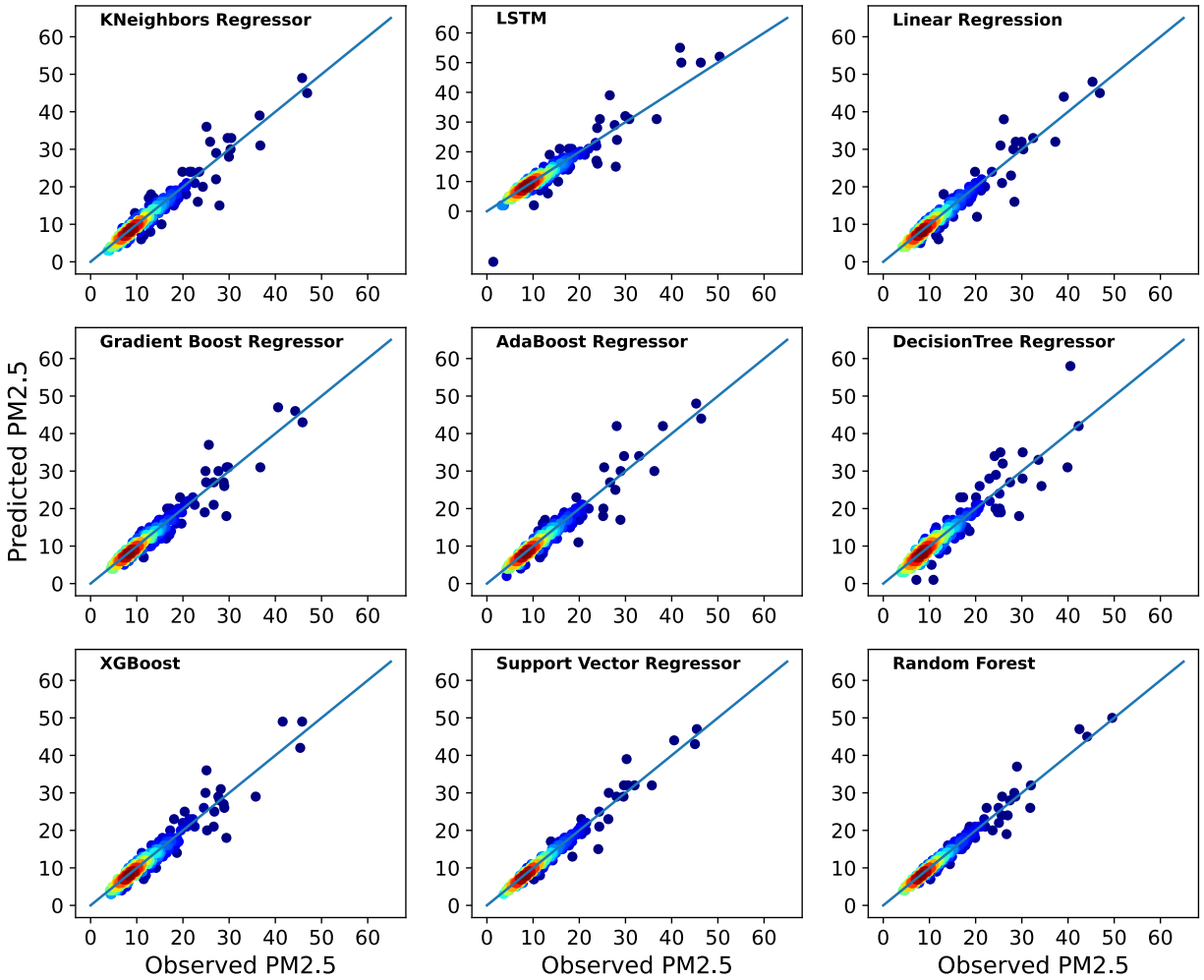

510

511 **Figure 5.** Scatter plots of observed and estimated daily $PM_{2.5}$ concentrations over California using
512 different machine learning models: (a) AdaBoost regressor, (b)DecisionTree regression, (c) Gradient
513 Boost regression, (d) Kneighbors regression (e) LSTM, (f) Linear regression, (g) Random Forest, (h)
514 Support Vector regression, and (I) XGBoost.
515

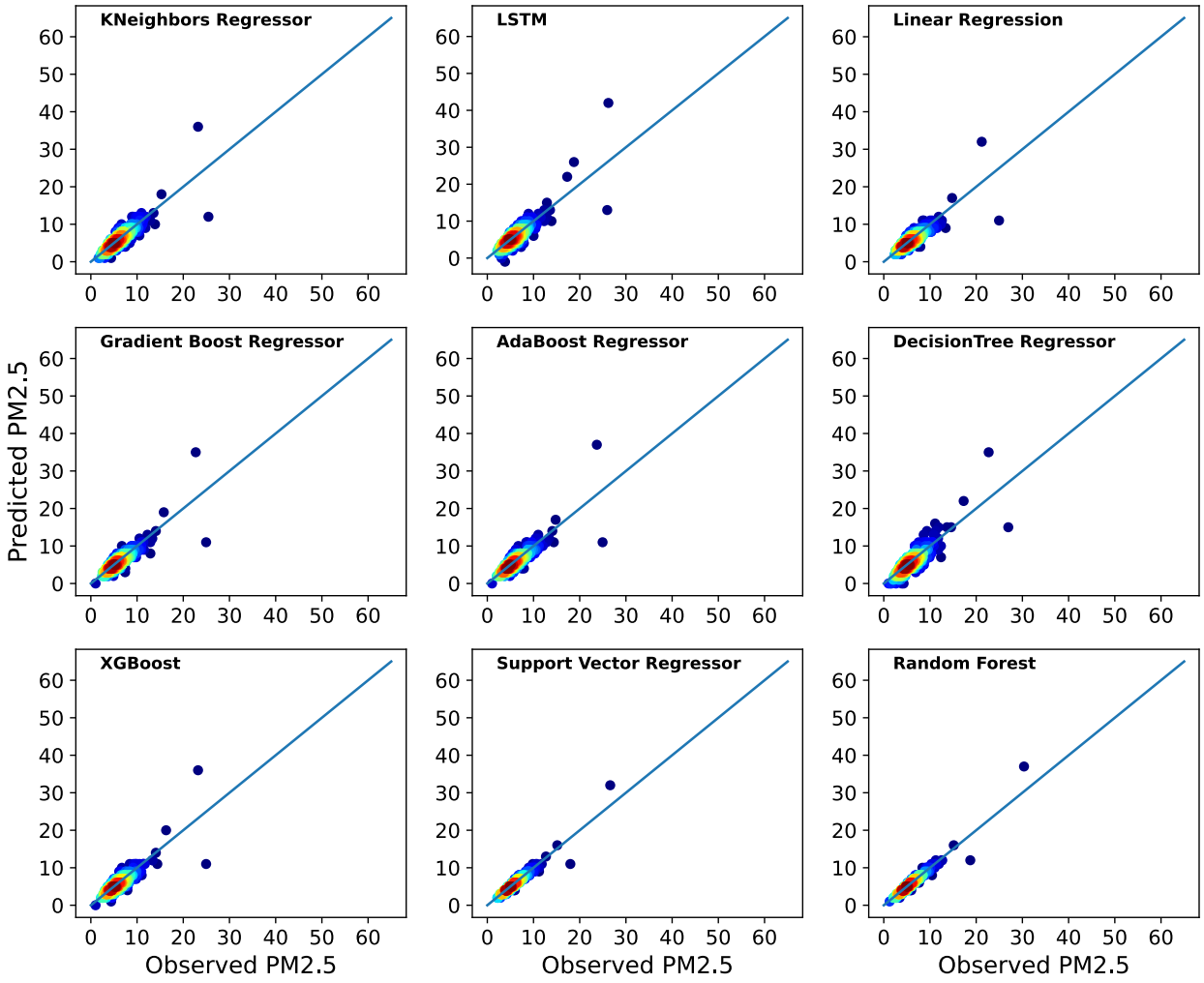

516

517 **Figure 6**. Scatter plots of observed and estimated daily $PM_{2.5}$ concentrations over New York using
518 different machine learning models: (a) AdaBoost regressor, (b)DecisionTree regression, (c) Gradient
519 Boost regression, (d) Kneighbors regression (e) LSTM, (f) Linear regression, (g) Random Forest,
520 (h) Support Vector regression, and (I) XGBoost.

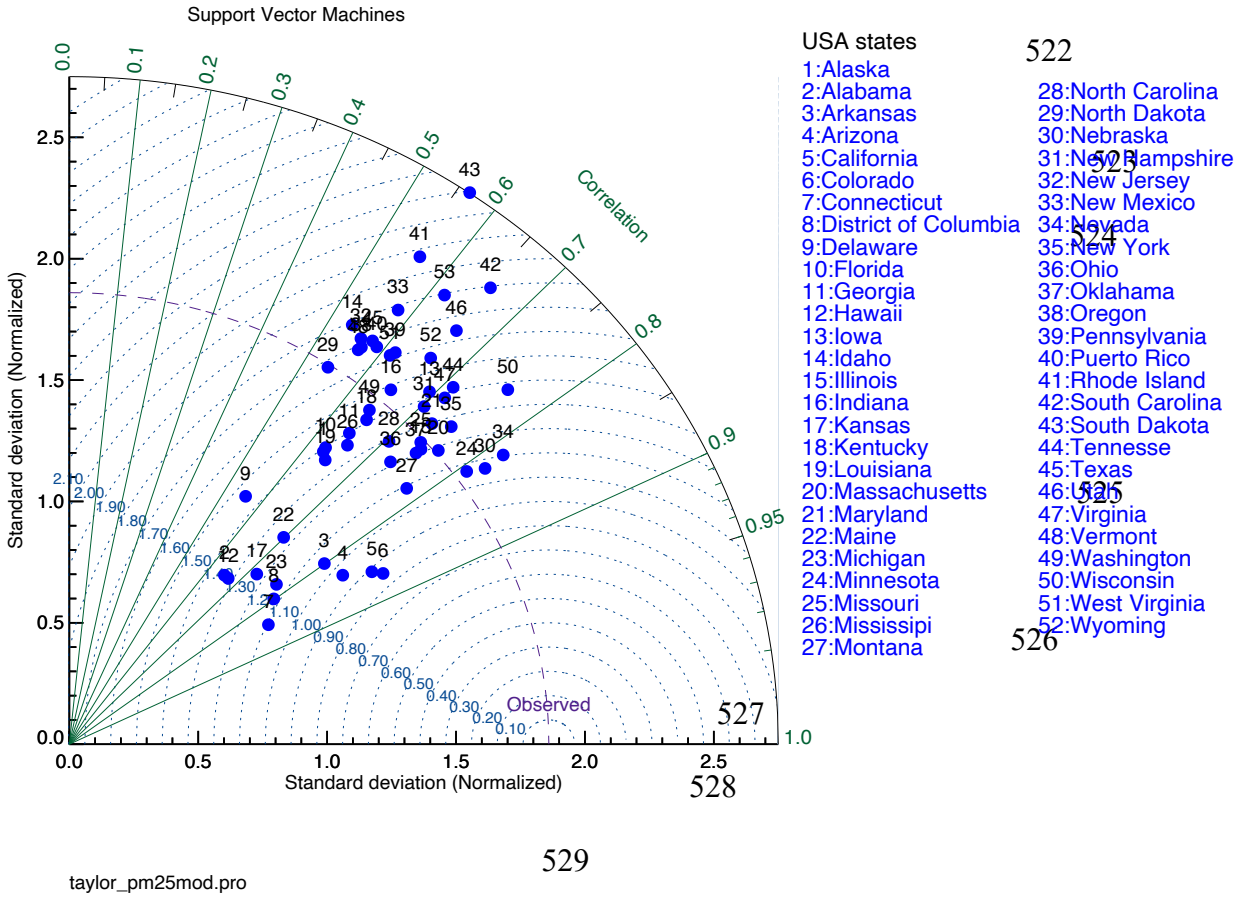

taylor_pm25mod.pro

Figure 7. Taylor diagram of the Support Vector Machines (SVM) over each state of the United States.

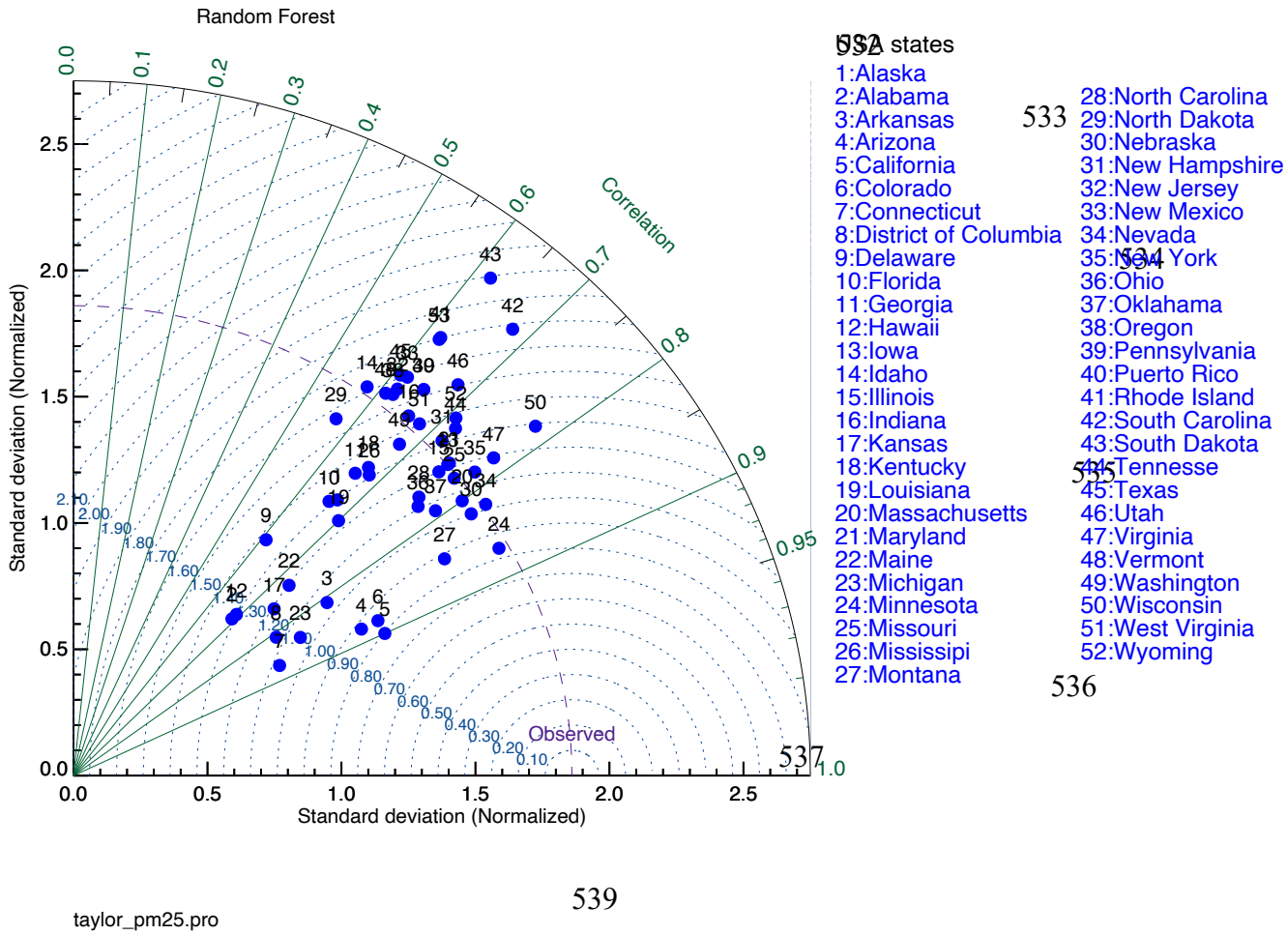

Figure 8. Taylor diagram of the Random Forest (RF) over each state of the United States.

Table 1: Different Model Metrics for New York State

New York								
Model	**RMSE**	**MAE**	**MAPE**	**R2**	**NSE**	**NORM**	**PBIAS**	**RSR**
Linear Regression	3.883	2.309	0.285	0.688	0.613	60.156	11.24	0.561
Decision Tree	5.136	3.109	0.254	0.454	0.533	79.58	13.44	0.691
Gradient Boost Regressor	3.822	2.394	0.545	0.698	0.683	59.207	8.210	0.546
AdaBoost Regressor	3.961	2.316	0.188	0.676	0.683	61.369	9.653	0.576
XG Boost	3.898	2.501	0.202	0.686	0.681	60.393	8.342	0.559
KNeighbors Regressor	3.919	2.379	0.195	0.683	0.677	60.711	7.515	0.562
LSTM	7.487	3.359	0.218	0.158	0.455	115.991	6.020	0.812
Random Forest	3.121	2.122	0.182	0.899	0.811	38.671	2.989	0.331
SVM	3.125	2.145	0.183	0.857	0.820	39.161	3.011	0.338

RMSE = Root mean squared error
MAE = Mean absolute error

MAPE = Mean absolute percentage error
R^2 = The coefficient of determination
NSE = Nash-Sutcliffe efficiency
PBIAS = Percent Bias
RSR = root mean square error ratio

Table 2: Different Model Metrics for California State

California								
Model	**RMSE**	**MAE**	**MAPE**	**R^2**	**NSE**	**NORM**	**PBIAS**	**RSR**
Linear Regression	3.695	2.599	0.326	0.43	0.694	57.243	12.086	0.932
Decision Tree	5.481	3.743	0.467	0.23	0.576	84.917	19.901	0.732
Gradient Boost Regressor	4.051	2.736	0.340	0.28	0.461	62.758	16.891	1.017
AdaBoost Regressor	3.804	2.636	0.342	0.33	0.435	58.938	17.532	0.969
XG Boost	4.271	2.972	0.372	0.17	0.438	66.178	18.726	1.075
KNeighbors Regressor	4.394	3.062	0.392	0.22	0.286	68.071	17.076	1.106
LSTM	5.025	3.252	0.339	0.46	0.309	77.853	18.027	0.618
Random Forest	3.051	2.233	0.315	0.77	0.817	46.894	7.022	0.355
SVM	3.714	2.618	0.320	0.71	0.897	47.853	7.027	0.424

RMSE = Root mean squared error
MAE = Mean absolute error
MAPE = Mean absolute percentage error
R^2 = The coefficient of determination
NSE = Nash-Sutcliffe efficiency
PBIAS = Percent Bias
RSR = root mean square error ratio